

Metallaborane Heteroatom Incorporation Reactions: Metallacarboranes, Metallathiaboranes, and an Iridaazaborane from Iridanonaborane Precursors

Jonathan Bould, Nigam P. Rath, and Lawrence Barton*

Department of Chemistry, University of Missouri—St. Louis, St. Louis, Missouri 63121

Received April 25, 1996[®]

Formation of metallaheteroboranes by insertion of heteroatoms into an existing metallaborane cluster, rather than adding the metal moiety to the heteroborane which is normally the case, has been achieved in the cases of carbon, nitrogen, and sulfur to produce nine-, ten-, and eleven-vertex metallaheteroborane clusters. Thus passage of acetylene through refluxing *p*-xylene solutions of either *arachno*-[(PMe₃)₂(CO)HirB₈H₁₂] (**1a**) or *nido*-[(PMe₃)₂(CO)IrB₈H₁₁] (**2a**) afforded the 11-vertex cluster *nido*-[9,9,9-(PMe₃)₂(CO)-9,7,8-IrC₂B₈H₁₁] (**5a**) in up to 44% yield. With the cage substituted species *arachno*-[(PMe₃)₂(CO)HirB₈H₁₁Cl] (**1b**), the analogous product is *nido*-[5-Cl-9,9,9-(PMe₃)₂(CO)-9,7,8-IrC₂B₈H₁₀] (**5b**) and the position of the Cl substituent in the product suggests that the acetylene moiety attacks across the open face of the intermediate *nido*-iridanonaborane species and that cage rearrangement does not occur during the course of the reaction. Similarly, reaction of **1a** with H₂S under identical conditions results in the formation *nido*-[2,2,2-(PMe₃)₂H-2,6-IrS₂B₈H₁₀] (**9a**), *closo*-[2,2,2-(PMe₃)₂H-2,1-IrS₂B₈H₈] (**10**), and *nido*-[(PMe₃)₂HirS₂B₈H₈] (**11a**) in overall yields of 13%, 7%, and 20%, respectively. Additionally, refluxing a solution of **1a** and anhydrous hydrazine in xylene afforded a 10% yield of the novel iridaazanaborane *nido*-[2,2,2-(PMe₃)₃-2,9-IrNB₇H₉] (**12**). The compound is the first metallazaanonaborane cluster to be described, and its formation indicates that methods similar to those used to generate azaboranes may be used on metallaboranes to generate metallazaboranes. In addition to characterization by a combination of ¹H, ³¹P, and ¹¹B NMR and IR spectroscopy and high-resolution mass spectrometry, single-crystal X-ray diffraction studies were carried out on compounds **5a**, **9a**, **10**, and **12**.

Introduction

Syntheses of metallaheteroborane clusters are typically effected by the addition of metal complexes to heteroborane clusters.¹ The most ubiquitous metallaheteroboranes are metallacarborane complexes although much work is being done on metalla complexes of thia,^{2,3} aza,⁴ and other heteroatom species, but herein we focus

only on those containing the atoms C, S, and N. Little attention has been given to the idea of producing metallaheteroborane clusters by the addition of the heteroatom to metallaborane clusters. Some carbon insertion products involving iridaboranes have been isolated in low yields as the unexpected degradation products from the reaction of Ir(CO)Cl(PPh₃)₂ and [B₁₀H₁₀]²⁻ in refluxing methanol, *viz.* [(PPh₃)(PPh₂P-C₆H₄)IrB₈H₆(OMe)C(OH)] and [(MeCOO)(PPh₃){HirCB₈H₇(PPh₃)}]⁵ and other work has been done on the reactions of iridadecaborane clusters with unsaturated molecules^{6a-c} although only one of these, to our knowl-

[®] Abstract published in *Advance ACS Abstracts*, November 1, 1996.

(1) (a) Grimes, R. N. *Chem. Rev.* **1992**, *92*, 251. (b) Hosmane, N. S.; Maguire, J. A. *J. Cluster Sci.* **1993**, *4*, 297. (c) Saxena, A. K.; Hosmane, N. S. *Chem. Rev.* **1993**, *93*, 1081. (d) Todd, L. J. In *Comprehensive Organometallic Chemistry*, If; Wilkinson, G., Abel, E. W., Stone, F. G. A., Eds.; Pergamon: London, 1995; Vol. 1, Ch. 8, pp 257–274.

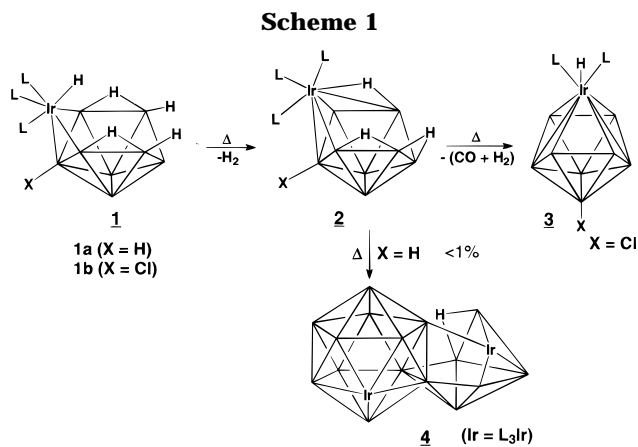
(2) Zimmerman, G. J.; Sneddon, L. G. *J. Am. Chem. Soc.* **1981**, *103*, 1102.

(3) (a) Kane, A. R.; Guggenberger, L. J.; Muettterties, E. L. *J. Am. Chem. Soc.* **1970**, *92*, 2571. (b) Siedle, A. R.; McDowell, D.; Todd, L. J. *Inorg. Chem.* **1974**, *13*, 2525. (c) Thompson, D. A.; Hilty, T. K.; Rudolph, R. W. *J. Am. Chem. Soc.* **1977**, *79*, 6774. (d) Hilty, T. K.; Thompson, D. A.; Butler, W. M.; Rudolph, R. W. *Inorg. Chem.* **1979**, *18*, 2642. (e) Base, K.; Štibr, B.; Zakharova, I. *Synth. React. Inorg. Metal. Org. Chem.* **1980**, *10*, 509. (f) Ferguson, G.; Hawthorne, M. F.; Kaitner, B.; Lalor, F. J. *Acta Crystallogr.* **1984**, *C40*, 1707. (g) Kang, S. O.; Carroll, P. J.; Sneddon, L. G. *Organometallics* **1988**, *7*, 772. (h) Kang, S. O.; Sneddon, L. G. *Inorg. Chem.* **1988**, *27*, 3769. (i) Ferguson, G.; Jennings, M. C.; Lough, A. J.; Coughlan, S.; Spalding, T. R.; Kennedy, J. D.; Fontaine, X. L. R.; Štibr, B. *J. Chem. Soc., Chem. Commun.* **1990**, 891. (j) Bown, M.; Fontaine, X. L. R.; Greenwood, N. N.; Kennedy, J. D. *Z. Anorg. Allg. Chem.* **1991**, *602*, 17. (k) Nestor, K.; Fontaine, X. L. R.; Greenwood, N. N.; Kennedy, J. D.; Thornton-Pett, M. *J. Chem. Soc., Dalton Trans.* **1991**, 2657. (l) Nestor, K.; Kennedy, J. D.; Thornton-Pett, M. *Inorg. Chem.* **1992**, *31*, 3339. (m) Coughlan, S.; Spalding, T. R.; Ferguson, G.; Gallagher, J. F.; Lough, A. J.; Fontaine, X. L. R.; Kennedy, J. D.; Štibr, B. *J. Chem. Soc., Dalton Trans.* **1992**, 2865. (n) Mazighi, K.; Carroll, P. J.; Sneddon, L. G. *Inorg. Chem.* **1992**, *31*, 3197. (o) Macias, R.; Holub, J.; Kennedy, J. D.; Štibr, B.; Thornton-Pett, M. *J. Chem. Soc., Chem. Commun.* **1994**, 2265.

(4) (a) Base, K.; Petrina, A.; Štibr, B.; Petricek, V.; Maly, K.; Linek, A. *Chem. Ind. (London)* **1979**, 212. (b) Base, K.; Bown, M.; Fontaine, X. L. R.; Greenwood, N. N.; Kennedy, J. D.; Štibr, B.; Thornton-Pett, M. *J. Chem. Soc., Chem. Commun.* **1988**, 1240. (c) Kester, G. J.; Huffman, J. C.; Todd, L. J. *Inorg. Chem.* **1992**, *31*, 3197. (d) Nestor, K.; Fontaine, X. L. R.; Greenwood, N. N.; Kennedy, J. D.; Thornton-Pett, M. Base, K.; Štibr, B. *Collect. Czech. Chem. Commun.* **1991**, *56*, 1607. (e) Hansen, H.-P.; Müller, J.; Englert, U.; Paetzold, P. *Angew. Chem., Int. Ed. Engl.* **1991**, *30*, 1377. (f) Paetzold, P.; Müller, J.; Meyer, F.; Hansen, H.-P.; Schneider, L. *Pure Appl. Chem.* **1994**, *66*, 255.

(5) Crook, J. E.; Greenwood, N. N.; Kennedy, J. D.; McDonald, W. S. *J. Chem. Soc., Chem. Commun.* **1983**, 83.

(6) (a) Bould, J.; Brint, P.; Fontaine, X. L. R.; Kennedy, J. D.; Thornton-Pett, M. *J. Chem. Soc., Chem. Commun.* **1989**, 1763. (b) Bould, J.; Brint, P.; Fontaine, X. L. R.; Kennedy, J. D.; Thornton-Pett, M. *J. Chem. Soc., Dalton Trans.* **1993**, 2335. (c) Coldicott, R. S. *Current Topics in the Chemistry of Boron*; Kabalka, G. W., Ed.; Special Publication; Royal Society of Chemistry: London, 1994; Vol. 143, p 297. (d) Ditzel, E. J.; Fontaine, X. L. R.; Greenwood, N. N.; Kennedy, J. D.; Sisan, Z.; Štibr, B.; Thornton-Pett, M. *J. Chem. Soc., Chem. Commun.* **1990**, 1741. (e) Nestor, K.; Fontaine, X. L. R.; Greenwood, N. N.; Kennedy, J. D.; Thornton-Pett, M. *J. Chem. Soc., Dalton Trans.* **1989**, 1465.



edge, has been reported to result in heteroatom insertion.^{6d,e} This latter example involves the incorporation of a RCN moiety into ruthena- and rhodadecaboranes, but it is less clear whether this reaction involves the metal center.

The iridanonaborane cluster *arachno*-[(PMe₃)₂(CO)-H]IrB₈H₁₁X] (X = H, **1a**; X = Cl, **1b**) is a unique example of a single metallaborane cluster compound which exhibits the classic *arachno* → *nido* → *closo* sequence (**1** → **2** → **3**, when X = Cl) of borane cluster chemistry.⁷ The clusters exhibit an orbital and electronic flexibility that involves proposed changes in both the formal oxidation state of the metal (Ir(III) to Ir(V) during **2** → **3**) and in the orbital interaction of the metal with the cluster {two (**1**) to three (**2**) to four (**3**) orbitals}.⁸ Conversely, when X = H, the *nido* → *closo* transition does not occur and low yields of larger clusters such as [(PMe₃)₂(CO)Ir]₂B₁₆H₁₄] (**1** → **2** → **4**) have been observed.⁹ Our initial studies on the work reported herein were based on the surmise that during the intracluster closure process (**1** → **3**) or intercluster condensation process (**1** → **4**) in which the iridium center essentially becomes more intimately bonded to the cluster, the iridium moiety would proceed through a transition state in which a coordinative site vacancy on the metal might be available to react with other, moderately nucleophilic species, rather than the cage itself. We chose to use acetylene rather than, for example, MeNC in order to reduce the possibility of simple ligand adduct formation although, in one case, as mentioned above, nitrile cage incorporation has been observed.⁶ Some products of cage insertion of carbon involving group 6^{10a} and 9^{10b} metallaboranes wherein carbonyl insertion effectively occurs have been observed. Related to this, orthocycloboronation reactions have been observed in iridaborane and other metallaborane clusters in which the H atom and the associated electron pair in the aryl CH bond of PPh₃ ligands on the metal are added to a boron vertex in the cluster suggesting that the metal vertex

could play a direct role in the interaction of borane clusters and unsaturated organic nucleophiles.¹¹ Important in the context of this report are reactions of alkynes and alkenes with metallaboranes in which reaction appears to take place at the metal center. Aromatization of norbornadiene at a Rh center in a rhodacarborane has been observed,¹² and recently reactions involving metal promoted alkyne^{13a} and norbornadiene^{13b} insertion into BH bonds have been described although carbon cluster incorporation was not observed in either case. Metallacarboranes are formed by the insertion of C₂H₂ into 2-(η^5 -C₅H₅)CoB₄H₈ in a reaction analogous to the insertion of C₂H₂ into B₅H₉¹⁴ and photolytic methods have also yielded carbon insertion products, viz. (CH₃)₄C₄B₄H₄ from the photolysis of B₄H₈-Fe(CO)₃ with CH₃C:CCH₃.¹⁵ Also pertinent to this discussion is the pyrolytic incorporation of the (C₅H₅) moiety and cluster expansion in [(η^5 -C₅H₅)₂HMo(η^2 -B₂H₅)] to give [CpMo(η^3 : η^2 -C₃H₃)C₂B₉H₉].¹⁶ Various other low-yield carbon insertions related to this latter report have been observed. This article reports the incorporation of a C₂ unit into an iridanonaborane and also the incorporation of both one and two S atoms and also a N atom into an iridanonaborane.

Experimental Section

Solvents used were reagent grade and were dried before use. *p*-Xylene was dried by refluxing and storage over NaH. Reactions were carried out under a nitrogen atmosphere and products were isolated in air using thin layer chromatography (TLC) on 20 × 20 cm glass plates coated with 0.1 cm of silica gel (Aldrich standard grade with gypsum binder and fluorescent indicator). Acetylene gas and H₂S were commercial grade in cylinders. *arachno*-(PMe₃)₂(CO)H]IrB₈H₁₂] (**1a**) and *arachno*-(PMe₃)₂(CO)H]IrB₈H₁₀Cl] (**1b**) were prepared according to the literature method^{8b} although extra purification steps in the preparation of *trans*-Ir(CO)Cl(PMe₃)¹⁷ used in the synthesis of the metallaborane resulted in a yield of 41% compared to 30% previously of *arachno*-(PMe₃)₂(CO)H]IrB₈H₁₂] and a concomitant reduced yield of the Cl-substituted analogue. *nido*-(PMe₃)₂(CO)IrB₈H₁₁] (**2a**)^{8c} was prepared by heating the *arachno*-iridanonaborane in a tube under vacuum at 400 ± 2 K for ca. 1 h followed by the addition of a minimum quantity of cold CHCl₃ to give a colorless solution containing the *nido* component as an almost white powder which may be recovered by filtration. Remaining traces of **1a** in the filtrate were recycled or purified by TLC. NMR spectroscopy was carried out on a Bruker ARX 500 spectrometer at 500.1 MHz for proton and 160.5 MHz for boron-11 and 202.5 MHz for ³¹P. Chemical shifts are reported in ppm for CDCl₃ solutions unless otherwise stated to low field (high frequency) of Et₂O·BF₃ for ¹¹B, of SiMe₄ for ¹H, and of 85% H₃PO₄ for ³¹P. High-resolution mass spectra (HRMS) were recorded at the Analytical Sciences

(7) (a) Williams, R. E. *Adv. Inorg. Chem. Radiochem.* **1976**, *18*, 67. (b) Rudolph, R. W. *Acc. Chem. Res.* **1976**, *9*, 446.

(8) (a) Bould, J.; Crook, J. E.; Greenwood, N. N.; Kennedy, J. D.; McDonald, W. S. *J. Chem. Soc., Chem. Commun.* **1982**, 346. (b) Bould, J.; Crook, J. E.; Greenwood, N. N.; Kennedy, J. D. *J. Chem. Soc., Dalton Trans.* **1984**, 1903. (c) Bould, J.; Greenwood, N. N.; Kennedy, J. D. *J. Chem. Soc., Dalton Trans.* **1984**, 2477.

(9) Barton, L.; Bould, J.; Kennedy, J. D.; Rath, N. P. *J. Chem. Soc., Dalton Trans.* **1996**, 3145.

(10) (a) Wegner, P. A.; Guggenberger, L. J.; Mutterties, E. L. *J. Am. Chem. Soc.* **1970**, *92*, 3473. (b) Crook, J. E.; Greenwood, N. N.; Kennedy, J. D.; McDonald, W. S. *J. Chem. Soc., Chem. Commun.* **1981**, 933.

(11) (a) Crook, J. E.; Greenwood, N. N.; Kennedy, J. D.; McDonald, W. S. *J. Chem. Soc., Chem. Commun.* **1981**, 933. (b) Crook, J. E.; Greenwood, N. N.; Kennedy, J. D.; McDonald, W. S. *J. Chem. Soc., Chem. Commun.* **1982**, 383. (c) Bould, J.; Greenwood, N. N.; Kennedy, J. D.; McDonald, W. S. *J. Chem. Soc., Chem. Commun.* **1982**, 465.

(12) Speckman, D. M.; Knobler, C. B.; Hawthorne, M. F. *Organometallics* **1985**, *4*, 1692.

(13) (a) Brauers, G.; Dossett, S. J.; Green, M.; Mahon, M. F. *J. Chem. Soc., Chem. Commun.* **1995**, 985. (b) Green, M.; Howard, J. A. K.; James, A. P.; Nunn, C. M.; Stone, F. G. A. *J. Chem. Soc., Dalton Trans.* **1987**, 61.

(14) Weiss, R.; Bowser, J. R.; Grimes, R. N. *Inorg. Chem.* **1978**, *17*, 1522.

(15) (a) Fehlner, T. P. *J. Am. Chem. Soc.* **1977**, *99*, 8355. (b) Fehlner, T. P. *J. Am. Chem. Soc.* **1980**, *102*, 3424.

(16) Grebenik, D.; Green, M. L. H.; Kelland, M. A.; Leach, J. B.; Mountford, P. *J. Chem. Soc., Chem. Commun.* **1989**, 1397.

(17) Labinger, J. A.; Osborn, J. A. *Inorg. Synth.* **1978**, *18*, 64.

Center of the Monsanto Co., St. Louis, MO, on a Finnigan MAT-95 mass spectrometer in the FAB mode using a nitrobenzyl alcohol matrix and standardized with PEG1000. The masses reported are for the most abundant peak (100%) in the molecular ion envelope. Elemental analyses were carried out by Atlantic Microlabs Inc., Norcross, GA.

Reaction of *arachno*-(PMe₃)₂(CO)HrB₈H₁₂] (1a), *arachno*-(PMe₃)₂(CO)HrB₈H₁₁Cl] (1b), and *nido*-(PMe₃)₂(CO)-IrB₈H₁₁] (2) with Acetylene. Acetylene gas, direct from the cylinder, was passed through a 2-propanol/dry ice trap into a two neck flask fitted with a condenser and containing a 5 mL *p*-xylene solution of *arachno*-(PMe₃)₂(CO)HrB₈H₁₂] (1a) (79 mg, 0.17 mmol). The solution was degassed for 10 min and then heated to reflux for a further 40–45 min during which time the solution darkened. The solution was cooled, the solvent removed under vacuum, redissolved in CH₂Cl₂ and filtered through silica gel, and again reduced in volume, applied to a preparative TLC plate, and developed with 70% CH₂Cl₂/pentane. Two colorless bands, visible under UV illumination, were apparent; one, *R_f* 0.4, was identified as *nido*-(PMe₃)₂(CO)IrC₂B₈H₁₁] (5a). The compound was removed from the silica gel with CH₂Cl₂. Pentane was added to the filtrate to give analytically pure, off white crystals. [Anal. Obsd (calcd): C, 21.93 (21.88); H, 5.78 (5.92). Yield: 36 mg, 0.073 mmol, 44%. IR/cm⁻¹: ν(CO) 1998 (s), ν(BH) 2517 (s).] Single crystals, suitable for X-ray analysis were grown by diffusion of pentane into a CDCl₃ solution of the compound. 5a is air stable and sublimes at 150–200 °C *in vacuo*. A second band at *R_f* 0.1–0.2 was characterized as *nido*-(PMe₃)₃-IrC₂B₈H₁₁] [compound 6, HRMS (C₁₁H₃₈B₈IrP₃): *m/q* 542.2632 (obsd), 542.2615 (calcd)] by a comparison of the ¹H, ¹¹B, and ³¹P NMR spectra with those of 5a. In a similar reaction, 72 mg, 0.15 mmol, of *nido*-(PMe₃)₂(CO)IrB₈H₁₁] was allowed to react with acetylene to give 5a in 41% yield. Compound 6 was also detected and combined with the product from the previous reaction to give 8 mg, 0.015 mmol, *ca.* 5% yield per reaction. Small amounts of the known^{18,19} *isonido* cluster type [(PMe₃)₂-HrC₂B₈H₁₀] {7a: NMR (ppm) ¹¹B [1H] +50.6 [+7.53], +11.5 [+4.85], +1.8 [+2.16 {doublet, ³J(³¹P–¹H) = 13 Hz}], –7.4 [+1.32], –13.2 [–0.20], –22.3 [+1.80], –27.7 [+0.09], –45.8 [–2.75], Ir–H –7.83 {doublet of doublets, *J* = 17 and 30 Hz}, cage C–H +3.81, +3.76; HRMS, (C₈H₂₈B₈IrP₂) *m/q* 466.2147 (obsd), 466.2095 (calcd)} were also observed in the reaction products. Refluxing xylene solutions of 5a for *ca.* 1 h gave 7a in approximately 25% yield based on the amount of reactant consumed (38 mg of 5a gave 3.5 mg of 7a, and 24 mg of 5a was returned).

Similarly to the above acetylene was passed through a xylene solution of 25 mg of *arachno*-(PMe₃)₂(CO)HrB₈H₁₁Cl] (1b) and the resultant mixture separated by TLC using 60:40 CH₂Cl₂/pentane as the mobile phase giving a band at *R_f* 0.3 containing 14.5 mg of material. The band was examined by NMR and seen to be a mixture of two compounds. The mixture could not be separated by chromatographic methods. Addition of pentane to a CH₂Cl₂ solution gave two crystalline species consisting of clumps of well-formed yellow crystals surrounded by colorless thin platelets. Separation was achieved by manually removing the yellow crystals from the clumps under a microscope giving a small amount (1.5 mg) of the colorless material which was identified as *nido*-[9,9,9-(PMe₃)₂(CO)-9,7,8-IrC₂B₈H₁₀-(5-Cl)] {5b: IR/cm⁻¹ ν(CO) 2006 (s), ν(BH) 2485, 2535, 2577; HRMS showed two equal intensity fragmentation envelopes corresponding to the molecular ion C₉H₂₈B₈IrP₂OCl (*m/q* 528.1744 (obsd), 528.1731 (calcd)) and the molecular ion minus (CO + H) (499.1715 (obsd), 499.1704 (calcd)}. The yellow crystals identified as the *closo*-type cluster [(PMe₃)₂-

HrC₂B₈H₉Cl] (7b) have been characterized by a single-crystal X-ray diffraction study and reported independently.²⁰

Reaction of *arachno*-(PMe₃)₂(CO)HrB₈H₁₂] with 1-Heptyne. 1-Heptyne (110 μL, 0.83 mmol, Aldrich) was syringed into a toluene solution of 1a (40 mg, 0.085 mmol) and the mixture refluxed for 54 min during which time it changed from colorless to dark yellow. After cooling the solvent was removed and the residue redissolved in CH₂Cl₂ and separated by TLC using 60:40 CH₂Cl₂/pentane. A number of boron-containing bands were observed on the TLC plate under UV light only one of which, a colorless band at *R_f* 0.25 yielding a pale yellow oil soluble in pentane, has so far been identified and partially characterized as *nido*-(PMe₃)₂(CO)IrC₂B₈H₁₀-(C₅H₁₁)] {8, 13 mg, 0.022 mmol, *ca.* 25% yield; IR/cm⁻¹ ν(CO) 1989(s), ν(BH) 2512 (br) 2563 (sh); HRMS (C₁₄H₃₉B₈IrP₂O) *m/q* 563.2921 (obsd), 563.2911 (calcd) [N.B. The most abundant peak at *ca.* *m/q* 564 was obscured by overlapping PEG calibrant peak] and molecular ion minus (H + CO) 535.2942 (obsd), 535.2881 (calcd)}. Boron-11 and ¹H NMR showed that the oil contained an amount of what was apparently a *nido*-iridadicarbaundecaborane isomer which could not be removed by TLC methods and thus preventing the definitive characterization of the compound.

Reaction of *arachno*-(PMe₃)₂(CO)HrB₈H₁₂] and *nido*-(PMe₃)₂(CO)IrB₈H₁₁] with H₂S. Hydrogen sulfide gas, direct from the cylinder, was passed through a 5 mL *p*-xylene solution of 1a (58.5 mg, 0.12 mmol) for 10 min and then heated to reflux for a further 40–45 min during which time the solution turned slightly red and some material deposited on the sides of the vessel. The mixture was allowed to cool, the solvent removed under vacuum, redissolved in CH₂Cl₂, and filtered through silica gel. The filtrate was again reduced in volume, applied to a preparative TLC plate and developed with 70% CH₂Cl₂/pentane. A number of almost colorless bands, visible under UV illumination were apparent. Among these, A, *R_f* 0.8, was identified as *nido*-[2,2,2-(PMe₃)₂H-2,6-IrSB₈H₁₀] [9a, 5 mg, 13% yield (all yields based amount of iridanonaborane consumed); mass spectrometry showed the molecular ion with loss of H₂, *m/q* (C₆H₂₇B₈IrP₂S) 472.1674 (obsd), 472.1736 (calcd)]. Crystals of the product formed in CDCl₃ NMR solution when stored in the refrigerator overnight. A second band B, *R_f* 0.7, was isolated and identified as *nido*-(PMe₃)₂-HrS₂B₈H₈] (11a, 9 mg 20% yield, HRMS for C₆H₂₇B₈IrP₂S₂ *m/q* 504.1409 (obsd) 504.1456 (calcd). ¹¹B NMR showed minor amounts of other species associated with B. A third band C, *R_f* 0.5, was identified as *closo*-[2,2,2-(PMe₃)₂H-2,1-IrSB₈H₈] [10, 2.6 mg, 7%; HRMS shows the molecular ion minus H, *m/q* (C₆H₂₆B₈IrP₂S) 471.1633 (obsd) 471.1658 (calcd)]. Finally, a band D, *R_f* 0.4, identified as the starting material *nido*-(PMe₃)₂(CO)IrB₈H₁₁] (20.5 mg, 35%) was isolated.

Each of the metallathiaborane compounds was found to react cleanly with the CDCl₃ NMR solvent, slowly at room temperature and more rapidly at elevated temperatures. A CDCl₃ solution of compound 9a was left in a water bath at 50 °C for 4 days and showed *ca.* 60% conversion to product. TLC in 70% CH₂Cl₂/pentane showed two bands, the first at *R_f* 0.8 due to 9a and the second, a pale yellow band at *R_f* 0.3, identified as *nido*-[2,2,2-(PMe₃)₂Cl-2,6-IrSB₈H₁₀] (9b). Pale yellow crystals were obtained from CH₂Cl₂/pentane solution. Mass spectroscopy showed two ion envelopes normalized to relative intensities of *ca.* 40% and 100%. The former was probably due to compound 9b with loss of H [*m/q* for C₆H₂₇B₈IrP₂SCl 508.1422 (obsd), 508.1410 (calcd)], and the latter, due to the molecular ion with loss of HCl [*m/q* for C₆H₂₆B₈IrP₂S 472.1724 (obsd), 472.1736 (calcd)].

The chloro-substituted derivative of compound 11a was isolated similarly giving pale yellow crystals, *R_f* 0.3, as *nido*-(PMe₃)₂ClIrS₂B₈H₈] (11b). HRMS gave two envelopes of equal

(18) Jung, C. W.; Hawthorne, M. F. *J. Am. Chem. Soc.* **1980**, *102*, 3024.

(19) Nestor, K.; Fontaine, X. L. R.; Greenwood, N. N.; Kennedy, J. D.; Plessek, J.; Stübr, B.; Thornton-Pett, M. *Inorg. Chem.* **1989**, *28*, 2219.

(20) Bould, J.; Rath, N. P.; Barton, L. *Acta Crystallogr., Sect. C*, in press.

Table 1. Crystal Data and Structure Refinement for Compounds **5a**, **9a**, **10**, and **12**

compd no.	5a	9a	10	12
empirical formula	C ₉ H ₂₅ B ₈ IrOP ₂	C ₆ H ₂₉ B ₈ IrP ₂ S	C ₆ H ₂₇ B ₈ IrP ₂ S	C ₁₀ H ₃₇ B ₇ IrCl ₃ NP ₃
fw	493.94	473.97	471.96	638.54
temp/K	295(2)	295(2)	295(2)	295(2)
cryst system	monoclinic	triclinic	triclinic	monoclinic
space group	<i>P</i> 2 ₁ / <i>n</i>	<i>P</i> 1	<i>P</i> 1	<i>P</i> 2 ₁
<i>a</i> /Å	8.769(3)	9.385(7)	9.046(3)	9.739(3)
<i>b</i> /Å	16.666(5)	9.485(7)	9.184(3)	9.865(2)
<i>c</i> /Å	13.511(4)	12.466(9)	12.508(8)	13.970(5)
α /deg	90	69.14(5)	70.66(4)	90
β /deg	97.12(2)	97.12(2)	74.90(4)	101.90(3)
γ /deg	90	63.63(3)	65.62(2)	90
<i>V</i> /Å ³	1959.3(11)	921.1(12)	883.8(7)	1313.3(2)
<i>Z</i>	4	2	2	2
<i>D</i> (calcd)/Mg/m ³	1.674	1.709	1.774	1.615
abs coeff/mm ⁻¹	6.967	7.511	7.828	5.569
cryst size/mm	0.5 × 0.3 × 0.2	0.4 × 0.2 × 0.1	0.4 × 0.5 × 0.1	0.03 × 0.1 × 0.5
<i>F</i> (000)	952	456	452	624
diffractometer used	Siemens P4(ST)	Siemens R3m	Siemens P4(ST)	Siemens P4(ST)
radiation used, Å	0.710 73	0.710 73	0.710 73	0.710 73
intensity collcn method	ω -2 θ	ω	ω	ω
θ range for data collcn/deg	1.95–30.60	1.76–27.51	1.74–27.57	2.14–25.07
index ranges	–12 ≤ <i>h</i> ≤ 12, 0 ≤ <i>k</i> ≤ 23, –17 ≤ <i>l</i> ≤ 19	–10 ≤ <i>h</i> ≤ 12–10 ≤ <i>k</i> ≤ 11, –15 ≤ <i>l</i> ≤ 16	–11 ≤ <i>h</i> ≤ 11–11 ≤ <i>k</i> ≤ 44, –16 ≤ <i>l</i> ≤ 16	–11 ≤ <i>h</i> ≤ 9, –9 ≤ <i>k</i> ≤ 10, –13 ≤ <i>l</i> ≤ 15
reflcs collcd	6016	7371	6888	2925
indepdt reflcs	5752 (<i>R</i> _{int} = 0.0433)	4157 (<i>R</i> _{int} = 0.0300)	4074 (<i>R</i> _{int} = 0.0681)	2448 (<i>R</i> _{int} = 0.0778)
data/restraints/params	5750/0/240	4153/0/213	4050/0/187	2445/1/137
goodness-of-fit on <i>F</i> ²	1.030	1.045	1.044	1.041
final <i>R</i> indices [<i>I</i> > 2 σ (<i>I</i>)]				
<i>R</i> ₁	0.0378	0.0298	0.0521	0.0882
<i>wR</i> ₂	0.0766	0.0774	0.1389	0.2509
largest diff peak and hole/e Å ⁻³	1.672 and –0.751	0.890 and –1.717	3.845 and –2.777	2.600 and –2.119

intensity (*m*/*q* (C₆H₂₆B₈IrP₂S₂Cl) 539.0860 (obsd), 539.1052 (calcd); low resln *m*/*q* [rel. intensity obsd (calcd)] 535 [20 (19)], 536 [44 (46)], 537 [75 (77)], 538 [98 (99)], 539 [100 (100)], 540 [73 (73)], 541 [36 (34)], 542 [18 (18)] and **11b** with loss of Cl (*m*/*q*, C₆H₂₆B₈IrP₂S₂ 503.1072 (obsd), 503.1378 (calcd); low resln *m*/*q* [rel. intensity obsd (calcd)] 500 [24 (22)], 501 [56 (52)], 502 [90 (84)], 503 [100 (100)], 504 [91 (90)], 505 [56 (53)], 506 [14 (11)]}.

Preparation of *nido*-[2,2,2-(PMe₃)₃-2,9-IrNB₇H₉] (12**).** To a dry, degassed xylene solution of **1a** (40 mg, 84 μmol) was added 0.054 mL of anhydrous hydrazine *via* syringe. The solution was heated to reflux for 40 min during which time a gray precipitate formed. After cooling, the solvent was removed and the mixture redissolved in CH₂Cl₂ and filtered giving 31.4 mg of insoluble solid. The filtrate was reduced in volume, applied to a preparative TLC plate, and developed using 70/30 CH₂Cl₂/pentane. A number of bands were apparent under UV illumination only one of which, the strongest, was amenable to isolation and was characterized as the title compound *nido*-[2,2,2-(PMe₃)₃-2,9-IrNB₇H₉] (**12**) (4.0 mg, 8 μmol, 10% yield, IR ν (BH) 2540, 2493 cm⁻¹) as an air-stable colorless crystalline solid. The high-resolution FAB mass spectrum for **12** showed two strong, almost equal intensity, envelopes corresponding to the molecular ion for **12** (C₉H₃₆IrB₇NP₃, *m*/*q* 519.2420 (obsd), 519.2390 (calcd)) and **12** with loss of (PMe₃ + H): (C₆H₂₆IrB₇NP₂, 442.1859 (obsd), 442.1869 (calcd)). NMR data are listed in Table 12. Crystals suitable for single-crystal X-ray diffraction purposes could only be grown from diffusion of pentane into a CHCl₃ solution of the compound although these tended to suffer from solvent loss following isolation.

X-ray Diffraction Analyses. A summary of crystal data, intensity data collection, and structure refinement parameters for compounds **5a**, **9a**, **10**, and **12** is listed in Table 1.

***nido*-[(PMe₃)₂(CO)IrC₂B₈H₁₁] (**5a**).** For compound **5a** data reduction and structure solution were carried out using the SHELXTL-PLUS (VMS) software package.²¹ Least-squares

refinement was achieved by using SHELXTL-5.0,²² and the empirical absorption correction was applied to the data using ψ -scan reflections.²² The structure was solved by the Patterson method and refined successfully in the space group *P*2₁/*n*. Full-matrix least-squares refinement was carried out by minimizing $\sum w(F_o^2 - F_c^2)^2$. The non-hydrogen atoms were refined anisotropically to convergence. All hydrogen atoms connected to boron atoms, including the single bridging hydrogen, were located from the difference Fourier synthesis and were refined isotropically. The methyl hydrogens were refined using a riding model. Selected interatomic distances and angles are listed in Table 2.

***nido*-[(PMe₃)₂HlrSB₈H₁₀] (**9a**).** Data reduction was carried out using XDISK, and structure solution and refinement were carried out using the SHELXTL-PLUS (5.0) software package.²² Absorption correction was applied to the data using equivalent reflections and ψ scan reflections (SHELXA).²³ The structure was solved by the Patterson method and refined successfully in the space group *P*1. The non-hydrogen atoms were refined anisotropically to convergence. All hydrogen atoms in the boron cage were located from difference Fourier syntheses and were refined isotropically. The methyl group H atoms were refined using a riding model. The hydride H was located and included in the final refinement. Geometrical parameters are listed in Table 6.

***closo*-[(PMe₃)₂HlrSB₈H₈] (**10**).** Data reduction was carried out using XSCANS. Structure solution and refinement was achieved as above for **9a**. All the hydrogen atoms in the boron cage were located from difference Fourier syntheses and were refined isotropically. The methyl group H atoms were refined using a riding model. It should be noted that the hydride atom H(2) was refined but it has a very short contact to the Ir atom of 1.36 Å and thus its reliability is questionable. Geometrical parameters are given in Table 8.

(22) Sheldrick, G. M. Siemens Analytical X-Ray Division, Madison, WI, 1994.

(23) Sheldrick, G. M. University of Göttingen, Germany.

(24) Sheldrick, G. M. Siemens Analytical X-Ray Division, Madison, WI, 1995.

(21) Sheldrick, G. M. Siemens Analytical X-Ray Division, Madison, WI, 1991.

Table 2. Selected Interatomic Distances (Å) and Angles (deg) for **5a**

Ir(9)–C(9)	1.870(6)	B(3)–B(4)	1.768(13)
Ir(9)–C(8)	2.182(7)	B(4)–C(8)	1.733(10)
Ir(9)–B(4)	2.232(7)	B(4)–B(5)	1.833(10)
Ir(9)–B(10)	2.235(6)	B(5)–B(10)	1.779(9)
Ir(9)–B(5)	2.239(7)	B(3)–C(8)	1.715(10)
Ir(9)–P(2)	2.331(2)	B(3)–C(7)	1.722(11)
Ir(9)–P(1)	2.341(2)	B(5)–B(6)	1.790(11)
B(1)–B(3)	1.748(13)	B(6)–B(11)	1.767(12)
B(1)–B(2)	1.753(14)	B(6)–B(10)	1.769(10)
B(1)–B(6)	1.771(11)	C(7)–C(8)	1.568(9)
B(1)–B(5)	1.780(12)	C(7)–B(11)	1.642(10)
B(1)–B(4)	1.786(11)	B(10)–B(11)	1.817(10)
B(2)–C(7)	1.703(11)	B(10)–H(101)	0.90(8)
B(2)–B(3)	1.732(11)	B(11)–H(101)	1.00(8)
B(2)–B(6)	1.734(12)	C(9)–O	1.153(8)
B(2)–B(11)	1.762(12)		
C(9)–Ir(9)–C(8)	93.3(3)	C(7)–B(3)–B(4)	102.9(5)
C(9)–Ir(9)–B(4)	89.6(3)	C(8)–B(4)–B(3)	58.6(4)
C(8)–Ir(9)–B(4)	46.2(3)	O–C(9)–Ir(9)	178.0(7)
C(9)–Ir(9)–B(10)	172.9(3)	C(8)–B(4)–B(1)	103.7(6)
C(8)–Ir(9)–B(10)	82.3(3)	C(8)–B(4)–B(5)	104.9(5)
B(4)–Ir(9)–B(10)	83.3(3)	C(8)–B(4)–Ir(9)	65.4(3)
C(9)–Ir(9)–B(5)	126.9(3)	B(3)–B(4)–Ir(9)	119.0(5)
C(8)–Ir(9)–B(5)	79.5(3)	B(1)–B(4)–Ir(9)	118.3(4)
B(4)–Ir(9)–B(5)	48.4(3)	B(5)–B(4)–Ir(9)	66.0(3)
B(10)–Ir(9)–B(5)	46.9(2)	B(10)–B(5)–Ir(9)	66.4(3)
C(9)–Ir(9)–P(2)	88.3(2)	B(1)–B(5)–Ir(9)	118.2(4)
C(8)–Ir(9)–P(2)	164.2(2)	B(6)–B(5)–Ir(9)	117.3(4)
B(4)–Ir(9)–P(2)	118.2(2)	B(4)–B(5)–Ir(9)	65.6(3)
B(10)–Ir(9)–P(2)	94.4(2)	C(8)–C(7)–B(11)	114.0(5)
B(5)–Ir(9)–P(2)	87.0(2)	C(8)–C(7)–B(2)	112.2(6)
C(9)–Ir(9)–P(1)	96.0(2)	B(11)–C(7)–B(2)	63.5(5)
C(8)–Ir(9)–P(1)	96.4(2)	C(8)–C(7)–B(3)	62.6(4)
B(4)–Ir(9)–P(1)	142.5(2)	B(11)–C(7)–B(3)	114.4(6)
B(10)–Ir(9)–P(1)	90.0(2)	B(2)–C(7)–B(3)	60.8(5)
B(5)–Ir(9)–P(1)	136.9(2)	C(7)–C(8)–B(3)	63.1(5)
P(2)–Ir(9)–P(1)	99.06(6)	C(7)–C(8)–B(4)	111.5(5)
C(7)–B(2)–B(3)	60.2(4)	B(3)–C(8)–B(4)	61.7(5)
C(7)–B(2)–B(6)	104.6(5)	C(7)–C(8)–Ir(9)	119.7(4)
C(7)–B(2)–B(1)	105.2(5)	B(3)–C(8)–Ir(9)	124.5(5)
C(7)–B(2)–B(11)	56.5(4)	B(4)–C(8)–Ir(9)	68.4(3)
C(8)–B(3)–C(7)	54.3(4)	B(6)–B(10)–Ir(9)	118.5(4)
C(8)–B(3)–B(2)	104.0(5)	B(5)–B(10)–Ir(9)	66.7(3)
C(7)–B(3)–B(2)	59.1(5)	B(11)–B(10)–Ir(9)	111.3(4)
C(8)–B(3)–B(1)	106.1(6)	C(7)–B(11)–B(2)	59.9(4)
C(7)–B(3)–B(1)	104.6(5)	C(7)–B(11)–B(6)	105.7(6)
C(8)–B(3)–B(4)	59.7(4)	C(7)–B(11)–B(10)	109.7(5)

nido-[(PMe₃)₃IrNB₈H₉] (12). Data reduction was carried out using XSCANS, and structure solution and refinement were carried out using SHELXTL-PLUS (5.03) software.²⁴ An absorption correction was applied to the data using equivalent reflections and ψ scan reflections (XEMP). The structure was solved by the Patterson method and refined successfully in the space group *P*2₁. The non-hydrogen atoms were refined anisotropically to convergence. The H atoms were refined using the appropriate riding model. Absolute configuration was determined by the Flack method (Flack x = 0.0095). Selected geometrical parameters are listed in Table 11.

Results and Discussion

Metallacarboranes. Passage of acetylene through refluxing *p*-xylene solutions of *arachno*-[(PMe₃)₂(CO)–HrB₈H₁₂] (**1a**, structure given in Scheme 1) with acetylene affords, after thin-layer chromatographic separation of the products, up to 44% yield of *nido*-[9,9,9-(PMe₃)₂(CO)-9,8,7-IrC₂B₈H₁₁] (**5a**, structure given in Scheme 2) according to eq 1. Similarly, the reaction

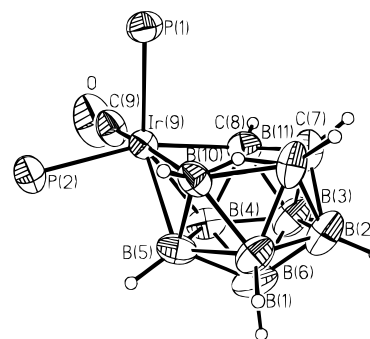
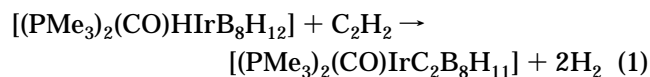


Figure 1. Molecular structure of *nido*-[9,9,9-(PMe₃)₂(CO)-9,8,7-IrC₂B₈H₁₁] (compound **5a**) with 50% probability thermal ellipsoids and with methyl groups omitted for clarity. All terminal boron hydrogen atoms and the bridging hydrogen atom $\mu\text{H}(10,11)$ were located and refined satisfactorily.

of acetylene with *nido*-[(PMe₃)₂(CO)IrB₈H₁₁] (**2**, structure given in Scheme 1) gives a 41% yield of **5a**, indicating that the initial *arachno*, **1a** to *nido*, **2a** cluster closure step plays no direct role in the acetylene incorporation mechanism. Also identified in both reactions were minor amounts of *nido*-[9,9,9-(PMe₃)₃-9,8,7-IrC₂B₈H₁₁] (**6**) in 5% yield. Compounds **5a** and **6**, which were obtained essentially pure in a combined yield of up to 49%, were identified by NMR and IR spectroscopy and, in the case of **5a**, by a single-crystal X-ray diffraction analysis (Figure 1). The NMR data for **5a** and **6** are listed in Table 3, and selected interatomic distances and angles for **5a** are listed in Table 2.

Species **5a** is clearly seen to be an 11-vertex *nido*-iridadicarbaundecaborane cluster incorporating two adjacent carbon atoms arising from the acetylene. The NMR data are in accord with the single crystal structural data, and the compound gives good ¹¹B–¹¹B COSY correlations although they were not sufficient to identify unambiguously the positions of the carbon atoms within the cluster. All interboron distances [ranging from 1.732(11) to 1.833(10) Å] are within the usual range, and the shorter distance between the carbon atoms, C(7)–C(8), of 1.568(9) Å is consistent with intercarbon distances in other metallacarboranes²⁵ confirming the atomic designations given. In addition to the terminal hydrogen atoms on the cage, the H atom bridging B(10)–B(11) was also located and refined.

In common with a broad range of *nido* metallaunderborane clusters of this type,²⁶ the molecule features a fluxionality on the NMR time scale in both its boron and proton spectra. The exchange process involves a rotation of the {(PMe₃)₂(CO)Ir} moiety with respect to the B(4)–B(5)–C(8)–B(10) face of the carborane cage as is also observed in the L₃RhC₂B₈H₁₁ analogues.¹⁸ The process was monitored by observation of the coalescence of the boron resonances assigned to vertex B(5) at δ -(¹¹B) +8.9 and +7.2 ppm which are in a relative intensity ratio of 2:1 giving an approximate value for the fluxional process of $\delta G^\ddagger(368 \text{ K})$ 71 kJ mol⁻¹. This

(25) For example see: (a) Barker, G. B.; Green, M.; Stone, F. G. A.; Welch, A. J. *J. Chem. Soc., Chem. Commun.* **1980**, 627. (b) Barker, G. B.; Godfrey, N. R.; Green, M.; Parge, H. E.; Stone, F. G. A.; Welch, A. J. *J. Chem. Soc., Chem. Commun.* **1983**, 277. (c) Lu, P.; Knobler, C. B.; Hawthorne, M. F. *Acta Crystallogr.* **1984**, C40, 1704. (d) Bown, M.; Fontaine, X. L. R.; Greenwood, N. N.; Kennedy, J. D.; Thornton-Pett, M. *Organometallics* **1987**, 6, 2254.

(26) See: Kennedy, J. D. *Prog. Inorg. Chem.* **1986**, 36, 211 (specifically pp 349–375).

Table 3. ^{11}B , ^1H , and $^{31}\text{P}^a$ NMR Data for *nido*-[(PMe_3) $_2$ (CO)IrC $_2$ B $_8$ H $_{11}$] (**5a**) in CDCl $_3$ (298 K) and CD $_3$ C $_6$ D $_5$ Solutions (353 K) and for *nido*-[(PMe_3) $_3$ IrC $_2$ B $_8$ H $_{11}$] (**6**) in CDCl $_3$ (298 K) Solution

assgnt	<i>nido</i> -[(PMe_3) $_2$ (CO)IrC $_2$ B $_8$ H $_{11}$] (5a) ^b				<i>nido</i> -[(PMe_3) $_3$ IrC $_2$ B $_8$ H $_{11}$] (6)			
	$\delta(^{11}\text{B})$ (353 K)	$\delta(^{11}\text{B})$ (298 K)	$J(\text{B}-\text{H})$ (298 K)	$\delta(^1\text{H})^c$ (298 K)	$^{11}\text{B}-^{11}\text{B}$ COSY correlns (353 K) ^d	$\delta(^{11}\text{B})$	$J(\text{B}-\text{H})$	$\delta(^1\text{H})^c$
2	+12.5	+11.3	148	+5.28	(3) <i>w</i> , (1,6) <i>s</i>	+9.2	130	+4.87
5	+8.9, [+7.2]	+8.3, [+6.1]	132 [134]	+3.55 ^j [+3.92]	(1,4,10) <i>s</i>	+7.7	129	+3.60 ^h
4	[-7.0], -10.9	[-7.3], -11.6	[140] 163	[+2.41], +2.46	(1,5) <i>s</i> , (3) <i>vw</i>	-9.6	140	+1.99 ⁱ
11	-12.2	-12.7	165	+2.60	(6) <i>s</i>	-14.2	131	+2.16
3	-17.9	-18.3	168	+2.38	(4) <i>vw</i> , (2) <i>w</i> , (1) <i>s</i>	-18.6	152	+2.09
10	-19.0	-19.8	141	+0.77	(5,6) <i>s</i>	-21.1	125	+0.50
6	-21.7	[-22.4], -22.7	130	+1.92	(1,2,5,10,11) <i>s</i>	-23.4	136	+1.57
1	-28.4	-29.3	138	+1.74	(2,3,4,5,6) <i>s</i>	-30.6	139	+1.26
<i>H</i> (10,11)				-4.35 [-3.78]				-4.02
<i>H</i> (7),(8)				+2.66 (2), [+2.97 (2)]				2.37, 2.40
<i>P</i> (CH $_3$)				1.87 [1.85], ^e 1.69 [1.65] ^f				1.74, ^g 1.58, ^g 1.54 ^g

^a ^{31}P NMR data in ppm (CD $_3$ C $_6$ D $_5$, 181 K): -41.1 (*s*), -46.9 (*s*), [-37.9, -49.2, $^2J(^{31}\text{P}-^{31}\text{P})$ 18 Hz]^b for compound **5a** and -46(*br*), -47.5, -49.9 (*d*, $J = 25.2$ Hz) for compound **6**. ^b Figures in brackets refer to the data for the minor rotamer component (see text). ^c Boron-proton resonances related by ($^{11}\text{B}-^1\text{H}$) HETCOR experiments for compound **3a** and (^1H)-(^{11}B {selective}) experiments for compound **6**. ^d *s* = strong, *m* = medium, *w* = weak. ^e $^2J(^{31}\text{P}-^1\text{H}) = 9.3$ [8.4] Hz. ^f $^2J(^{31}\text{P}-^1\text{H}) = 10.0$ [9.3] Hz. ^g $^2J(^{31}\text{P}-^1\text{H})$ 8.9 Hz. ^h Doublet, probably due to coupling to phosphorous, $^3J(^{31}\text{P}-^1\text{H})$ 22 Hz. ⁱ Doublet, probably due to coupling to phosphorous, $^3J(^{31}\text{P}-^1\text{H})$ 19 Hz. ^j Doublet, $^3J(^{31}\text{P}-^1\text{H})$ 22 Hz, probably due to *cisoidal*-coupling to P(2).

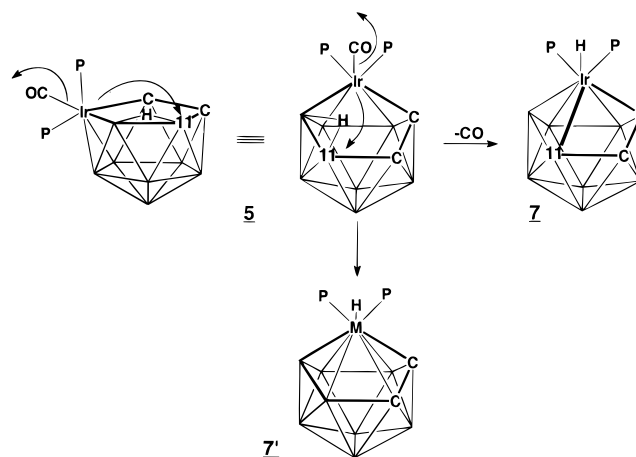
Table 4. ^{11}B , ^1H , and $^{31}\text{P}^a$ NMR Data for *nido*-[(PMe_3) $_2$ (CO)IrC $_2$ B $_8$ H $_{10}$ Cl] (**5b**, CDCl $_3$ Solution at 302 K)

assgnt	$\delta(^{11}\text{B})^b$	$\delta(^1\text{H})^b$	($^{11}\text{B}-^{11}\text{B}$) COSY correlns (323 K) ^c
5	+18.1	<i>d</i>	(1, 4, 6/10) <i>s</i>
2	+8.5	+4.63	(3) <i>vw</i> , (1, 6/10) <i>m</i>
4	-7.0	+2.51	(5) <i>s</i> , (1) <i>w</i>
11	-12.8	+2.47	(1, 6/10) <i>s</i>
3	-18.1	+2.25	(1, 6/10) <i>s</i>
6/10	-20.2 (2)	+1.90, +1.45	(2) <i>s</i> , (1, 11) <i>m</i>
1	-26.8	+1.70	(2, 4, 3, 6/10) <i>s</i> , (5) <i>w</i>
<i>H</i> (10,11)		-3.30	
<i>H</i> (7),(8)		2.30(2)	
(CH $_3$)		+1.85(9), +1.73(9) ^e	

^a ^{31}P NMR data (CDCl $_3$, 230 K): -35.0, -47.4 ppm, $^2J(^{31}\text{P}-^{31}\text{P})$ 14 Hz. ^b Relative intensities in parentheses. Boron-proton resonances related by ($^{11}\text{B}-^1\text{H}$) HETCOR experiments and ^1H -(^{11}B {selective}) decoupling experiments. ^c *s* = strong, *m* = medium, *w* = weak, *vw* = very weak. ^d Site of chlorine substituent. ^e Doublets, $^2J(^{31}\text{P}-^1\text{H})$ 9 Hz.

compares well to calculated values for related compounds such as *nido*-[(PPh_3) $_2$ (CO)IrB $_{10}$ H $_{11}$ (PPh_3)] (65 kJ mol $^{-1}$ at 319 K)^{27a} and *nido*-[(7,7,7-(PMe_2Ph) $_2$ PtB $_{10}$ H $_{11}$ (4-Cl)] (77 kJ mol $^{-1}$).^{27b} Presumably the solid-state structure (Figure 1) with the carbonyl group *cis* to C(8) represents the major rotamer component. In the chloro-substituted compound **5b** described below where the chlorine is in the B(5) position, the ^{31}P and the bridging hydrogen resonances (Table 4) have chemical shift values very close to those of the minor component in **5a** and there is no evidence of fluxionality up to 380 K suggesting that steric interaction with the PMe_3 ligand results in the alternate configuration for **5b**.

Compound **5a** (structure **5** in Scheme 2) may be compared to a similar rhodium species *nido*-(PPh_3) $_2$ -RhC $_2$ B $_8$ H $_{11}$ ^{25c} prepared more conventionally from the addition of the metal complex RhCl(PPh_3) $_3$ to the *nido*-carborane anion [C $_2$ B $_8$ H $_{11}$] $^-$. The major difference between the rhodium and iridium species lies in the coordinative unsaturation of the Rh species which undergoes a reversible addition of the metal to B(11) to afford what was the presumed to be *closo* species [(PPh_3) $_2$ HRhC $_2$ B $_8$ H $_{10}$] (structure type **7'**, Scheme 2) on the basis of NMR spectroscopy but which was later

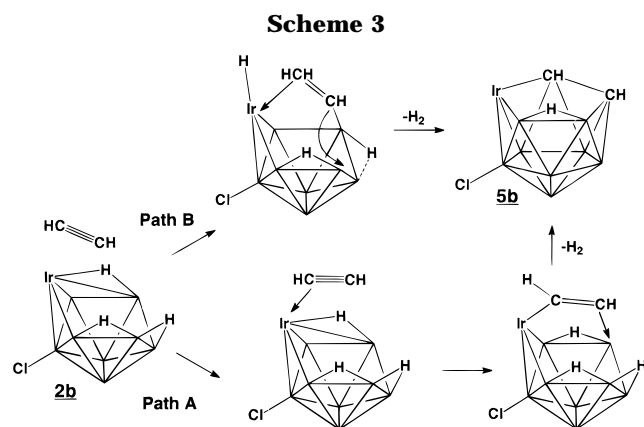
Scheme 2

shown to have an *isonido*-type structure with a four membered open face¹⁹ (structure type **7**, Scheme 2). In the case of **5a** a nonreversible carbonyl loss occurs (structures **5** \rightarrow **7**, Scheme 2) when refluxed for an extended period in xylene to give *isonido*-[(PMe_3) $_2$ -HrC $_2$ B $_8$ H $_{10}$], **7a**, in *ca.* 25% yield as illustrated in Scheme 2. The compound was characterized by NMR spectroscopy (see Experimental Section) and exhibits an equivalent cluster geometry to the rhodadicarbaundecaborane.

In an effort to obtain mechanistic information about the site of insertion of the C $_2$ moiety the reaction was repeated with the chloro-substituted iridanoborane *arachno*-[(PMe_3) $_2$ (CO)HrB $_8$ H $_{11}$ Cl] (**1b**). This compound is obtained in low yield as a byproduct in the preparation of the unsubstituted analogue (**1a**). The *nido*-iridanoborane formed on heating the *arachno* species (**1** \rightarrow **2**, Scheme 1) has been previously characterized by NMR spectroscopy,^{8c,28} and the chloro substituent is reasonably proposed to remain in its relative position during the *arachno* to *nido* transformation thereby providing a marker and supplying information on the mode of addition of the alkyne to the metallaborane cluster. Passage of acetylene through a refluxing solu-

(28) Beckett, M. A.; Bown, M.; Fontaine, X. L. R.; Greenwood, N. N.; Kennedy, J. D.; Thornton-Pett, M. *J. Chem. Soc., Dalton Trans.* **1988**, 1969.

(27) (a) See ref 26, p 353. (b) Reference 26, p 359.



tion of **1b** (25 mg) for 40 min followed by chromatographic separation of the reaction mixture resulted in the isolation of 14.5 mg of a mixture of two crystalline solids—the pale yellow *isonido*-type²⁰ compound $[\text{PMe}_3]_2\text{-HIrC}_2\text{B}_8\text{H}_9\text{Cl}$ (**7b**) and the colorless *nido*-[9,9,9-(PMe_3)₂(CO)-9,7,8- $\text{IrC}_2\text{B}_8\text{H}_{10}$ (5-Cl)] (**5b**). The structural characterization of **7b** is reported elsewhere.²⁰ The compounds were separated manually under a microscope, and thus the relative amounts were difficult to assess although we estimate them to be in a ratio of 60:40, respectively. The higher yield of the decarbonylated species compared to that for compound **1a** emphasizes the electronic effect on the metal vertex of the halogen substituent in **1b**. Compound **5b** (structure given in Scheme 3) was characterized by NMR and IR spectroscopy by comparison with compound **5a**. The position of the Cl substituent follows readily from [¹¹B–¹¹B] COSY NMR experiments (Table 4) which show a connectivity pattern for the singlet resonance at $\delta(^{11}\text{B})$ +18.1 ppm similar to that for the resonance at +8.9 ppm in **5a** assigned to cluster vertex B(5). The downfield shift of *ca.* 10 ppm is reasonable for a chlorine atom.²⁸ The position of the chlorine substituent in the product suggests that it is unlikely that isomerization has occurred during the reaction and the observed product may be rationalized by a simple addition of the acetylene moiety to the open face of the *nido*-iridaborane cluster at the metal atom.

The opening of a vacant coordination site on the metal during the thermolysis and coordination of the alkyne to the metal cluster followed by insertion of the β -carbon into the cluster (Scheme 3, path A, **2b** → **5b**) is a possible initial step. Metal–alkyne coordination has been observed in the related *nido*-iridaborane system where the species *nido*-[(PPh_3)($\text{PPh}_2\text{C}_6\text{H}_4$) $\text{HIrB}_9\text{H}_{12}$] combines with acetylene affording a small yield of the iridacyclopentadiene species *isocloso*-[($\text{PPh}_2\text{C}_6\text{H}_4$)(C_4H_4)- $\text{IrB}_9\text{H}_7(\text{PPh}_3)$].^{6a,b} In the latter case, after the initial addition of the alkyne, the tendency of iridium to lose or transfer the more weakly bound PPh_3 ligand to the cage opens a vacant coordination site and presumably allows the reaction to proceed via coordination of a second acetylene molecule rather than via C_2 incorporation as reported herein and, additionally, the migrating phosphine ligands effectively supply the extra electrons that any intermediate electron-deficient cluster might otherwise gain from the incoming alkyne moiety. A similar reaction with the PMe_3 ligated species might proceed quite differently. Alternatively, hydroboration

Table 5. ¹¹B, ¹H, and ³¹P^a NMR Data for *nido*-[(PMe_3)₂(CO) $\text{IrC}_2\text{B}_8\text{H}_{10}(\text{C}_5\text{H}_{11})$] (**8**) in C_7D_8 Solution at 373 K

assgnt	$\delta(^{11}\text{B})^b$	$\delta(^1\text{H})^b$	(¹¹ B– ¹¹ B) COSY correlns (353 K) ^c
2	+15.4	+5.73	(3) <i>w</i> , (1,6) <i>s</i>
5	+8.0	+4.01	(4) <i>w</i> , (6) <i>m</i> , (1,10) <i>s</i>
4	−9.6	+2.98	(1,5) <i>w</i>
11	−10.9	+2.99	(6) <i>s</i>
3	−15.3	+2.63	(4) <i>vw</i> , (2) <i>w</i> , (1) <i>s</i>
10	−18.6	+0.96	(5,6) <i>s</i>
6	−21.6	+2.62	(5) <i>m</i> , (1,2,10,11) <i>s</i>
1	−27.2	+2.42	(4) <i>w</i> , (2,3,5,6) <i>s</i>
H(10,11)		−3.85	
H(7) or (8)		<i>d</i>	
P(CH ₃) ^e		+1.90, +1.65	

^a ³¹P NMR data (CDCl_3 , 223 K). Resonances due to two rotamers apparent in *ca.* 1:1 ratio, −38.3, −44.9 ppm, ² $J(^{31}\text{P}–^{31}\text{P})$ 6 Hz, and −35.0, −47.4 ppm, ² $J(^{31}\text{P}–^{31}\text{P})$ 14 Hz. ^b Boron–proton resonances related by (¹¹B–¹H) HETCOR experiments and ¹H–{¹¹B(selective)} decoupling experiments. ^c *s* = strong, *m* = medium, *w* = weak, *vw* = very weak. ^d Doublets, ² $J(^{31}\text{P}–^1\text{H})$ 9 Hz. Broad multiplets due to C_5H_{11} substituent on C(7) or C(8) centered at +1.2 and +0.8 ppm (recorded at 223 K). ^e ² $J(^{31}\text{P}–^1\text{H})$ = 9.3 Hz.

of the alkyne,²⁹ by the metallaborane cluster, is also a possible initial step followed by coordination of the resultant alkenyl fragment to the metal vertex (Scheme 3, path B). However, in an attempted reaction of acetylene with *arachno*-[(PMe_2Ph)₂ $\text{PtB}_8\text{H}_{12}$], which might also be expected to undergo at least the initial hydroboration reaction, the only borane species we were able to identify was a low yield of the previously reported phosphine-substituted platinaborane *arachno*-[4,4-(PMe_2Ph)₂-4- $\text{PtB}_8\text{H}_{11}$ -6-(PMe_2Ph)],^{30a} which is a simple thermal degradative product from the thermolysis of *arachno*-[(PMe_2Ph)₂ $\text{PtB}_8\text{H}_{12}$].^{30b}

Presumably, if hydroboration were the initial step, then a substituted alkyne, RCCH , might be expected to undergo a normal anti-Markonikov addition and the R group would tend to be found adjacent to the metal in the product. In this vein we investigated the incorporation of the 1-substituted alkyne, 1-heptyne, into the iridaborane cluster. *nido*-[(PMe_3)₂(CO) $\text{IrC}_2\text{B}_8\text{H}_{10}(\text{C}_5\text{H}_{11})$] (**8**), identified from NMR (Table 5), IR spectroscopy, and high-resolution mass spectrometry, was isolated in *ca.* 25% yield together with the corresponding *isonido*-type product produced by loss of the metal carbonyl group. However, although **8** could be readily identified as a substituted analogue of **5a**, the position of the pendant alkyl group on the α or β cluster carbon atom could not be determined directly from NMR spectroscopy and the compound, as isolated, appeared to be an oil thus discounting the possibility of a structural determination. An inseparable, small amount of a closely related species was present in the product and resultant overlapping NMR resonances confused attempts to characterize the species unambiguously.

It is interesting to note the change in the nature of the H atom positions, when viewed from the point of view of the metal vertex and the open face of the cluster. As shown in Scheme 1 the terminal iridium hydride in compound **1** is effectively incorporated into the cluster in the form of an Ir–H–B bond on transformation to **2**

(29) Brown, H. C. *Boranes in Organic Chemistry*; Cornell University Press: Ithaca, NY, 1972; Chapter XV.

(30) (a) Salter, P. Ph.D. Thesis, University of Leeds, 1987. (b) Boocock, S. K.; Greenwood, N. N.; Hails, M. J.; Kennedy, J. D.; MacDonald, W. S. *J. Chem. Soc., Dalton Trans.* **1981**, 1415.

Table 6. Selected Interatomic Distances (Å) and Angles (deg) for **9a**

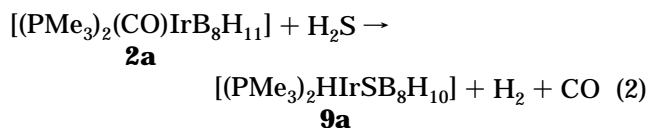
Ir(2)–B(3)	2.228(6)	B(1)–B(5)	1.767(9)
Ir(2)–B(1)	2.232(6)	B(1)–B(10)	1.797(9)
Ir(2)–B(5)	2.266(6)	B(1)–B(4)	1.815(9)
Ir(2)–B(7)	2.279(6)	B(1)–B(3)	1.873(9)
Ir(2)–P(1)	2.334(2)	B(1)–H(1)	1.27(5)
Ir(2)–P(2)	2.336(2)	B(4)–B(9)	1.726(10)
Ir(2)–S(6)	2.458(2)	B(7)–B(8)	1.936(9)
Ir(2)–H(2)	1.36(7)	B(8)–B(9)	1.770(10)
S(6)–B(7)	1.893(7)	B(8)–H(89)	1.32(7)
S(6)–B(5)	1.901(7)	B(9)–B(10)	1.764(10)
B(3)–B(7)	1.789(9)	B(9)–H(89)	1.25(7)
B(3)–B(8)	1.793(9)	B(9)–H(910)	1.37(7)
B(4)–B(8)	1.774(10)	B(10)–H(910)	1.27(7)
B(4)–B(10)	1.794(11)	B(3)–B(4)	1.801(10)
B(5)–B(10)	1.936(9)		
B(1)–Ir(2)–H(2)	86(3)	B(7)–S(6)–Ir(2)	61.6(2)
P(1)–Ir(2)–H(2)	89(3)	B(5)–S(6)–Ir(2)	61.1(2)
S(6)–Ir(2)–H(2)	163(3)	B(1)–B(5)–S(6)	116.7(4)
B(3)–Ir(2)–B(1)	49.7(2)	B(1)–B(5)–B(10)	57.8(4)
B(3)–Ir(2)–B(5)	80.3(2)	S(6)–B(5)–B(10)	113.1(4)
B(1)–Ir(2)–B(5)	46.2(2)	B(1)–B(5)–Ir(2)	65.8(3)
B(3)–Ir(2)–B(7)	46.8(2)	S(6)–B(5)–Ir(2)	71.7(2)
B(1)–Ir(2)–B(7)	80.5(2)	B(10)–B(5)–Ir(2)	118.5(4)
B(5)–Ir(2)–B(7)	76.8(2)	B(3)–B(7)–S(6)	116.1(4)
B(3)–Ir(2)–P(1)	150.7(2)	S(6)–B(7)–B(8)	113.8(4)
B(1)–Ir(2)–P(1)	103.0(2)	B(3)–B(7)–Ir(2)	65.1(3)
B(5)–Ir(2)–P(1)	86.0(2)	S(6)–B(7)–Ir(2)	71.5(2)
B(7)–Ir(2)–P(1)	152.4(2)	B(8)–B(7)–Ir(2)	117.6(3)
B(3)–Ir(2)–P(2)	104.1(2)	B(3)–Ir(2)–H(2)	80(3)
B(1)–Ir(2)–P(2)	152.3(2)	B(5)–Ir(2)–H(2)	128(3)
B(5)–Ir(2)–P(2)	151.3(2)	B(7)–Ir(2)–H(2)	119(3)
B(7)–Ir(2)–P(2)	85.7(2)	P(2)–Ir(2)–H(2)	80(3)
P(1)–Ir(2)–P(2)	100.40(6)	B(5)–B(1)–Ir(2)	67.9(3)
B(3)–Ir(2)–S(6)	83.5(2)	B(10)–B(1)–Ir(2)	127.3(4)
B(1)–Ir(2)–S(6)	83.4(2)	B(4)–B(1)–Ir(2)	121.2(4)
B(5)–Ir(2)–S(6)	47.2(2)	B(3)–B(1)–Ir(2)	65.1(3)
B(7)–Ir(2)–S(6)	46.9(2)	B(7)–B(3)–Ir(2)	68.1(3)
P(1)–Ir(2)–S(6)	105.81(7)	B(8)–B(3)–Ir(2)	127.4(4)
P(2)–Ir(2)–S(6)	104.45(7)	B(4)–B(3)–Ir(2)	122.1(4)
B(7)–S(6)–B(5)	96.1(3)	B(1)–B(3)–Ir(2)	65.3(3)

and, on addition of alkyne, the only remaining facial H atom is a B–H–B bridging hydrogen atom which then reverts to a terminal metal hydride in compound **7** (structure **7**, Scheme 2). This suggests that it would be interesting to prepare rhodium analogues of these compounds which might tend to exhibit features of reversibility.^{18,31}

Following the success of the alkyne reactions it became evident that other small molecules might be amenable to incorporation and, rather than cultivate the further chemistry of carborane formation at this stage, we chose to explore this possibility as is described in the next two sections.

Metallathiaboranes. Passage of H₂S through refluxing xylene solutions of **1a** followed by repeated TLC separation affords a number of metallathiaboranes in a combined yield of 40%. The first, isolated in 13% yield was identified by NMR spectroscopy and high-resolution mass spectroscopy together with a single-crystal X-ray diffraction study as *nido*-[2,2,2-(PMe₃)₂H-2,6-IrSB₈H₁₀] (compound **9a**). NMR data are listed in Table 7 together with data for the heteroborane analogue *nido*-[6-SB₉H₁₁]. Selected interatomic dimensions are listed in Table 6. A projection of the structure is shown in Figure 2. As with the previous alkyne reactions we repeated the experiment with the *nido*-iridanonorane compound **2** and obtained the similar results although subsequently, for convenience, we used the *arachno*

complex. Compound **9a** clearly results, after initial dihydrogen loss in the *arachno*-**1a** → *nido*-**2a** step, from addition of H₂S to the *nido*-iridanonorane with dihydrogen and carbonyl elimination according to eq 2. It



would appear that CO elimination is a key step in providing a coordination site on the Ir for attack by the sulfur atom, if indeed the incorporation of sulfur is metal-centered. The cluster is the first metallaborane analogue of the thiadecaborane *nido*-[SB₉H₁₁] with the sulfur in the prow position in the open face of the cage and the iridium in the adjacent basal 2-position. The NMR data for **9a** (Table 7) are completely in accord with the structural information and show, with allowance for the effect of the metal atom, a similar shielding pattern and COSY connectivity pattern to that of *nido*-SB₉H₁₁³² in contrast to those of the only other metallathiadecaborane analogues known all of which exhibit *arachno* structures as typified by [9,9-(PPh₃)₂-6,9-PtSB₈H₁₀].^{33a} An analogue of **9a**, [2- $\{\eta^6\text{-C}_6\text{Me}_3\text{H}_3\}$ Fe-6-OB₈H₁₀], has been structurally characterized but was obtained only in trace quantities, and NMR data are unavailable.^{33b} Consistent with the *nido* descriptor for **9a**, the B(5)–B(10) and B(7)–B(8) distances of 1.936(9) Å are the longest cluster interboron distances mirroring those in decaborane(14) itself, obtained in a neutron diffraction study (1.973(4) Å).³⁴ Unfortunately the structure of *nido*-SB₉H₁₁ has not been reported so a structural comparison is not possible. The structure of the related species *arachno*-[9-(Et₃N)-SB₉H₁₁] is available,³⁵ but the corresponding B–B bonds are H-bridged rendering comparisons less useful. The B(5)–B(10)/B(7)–B(8) distances contrast those in the platinathiadecaborane in which they exhibit the more normal interboron distances of ca. 1.845 Å³³ as has been discussed elsewhere.³⁶

A comparison of the boron shielding patterns for the related species *nido*-B₁₀H₁₄,³⁷ *nido*-SB₉H₁₁,³² *nido*-[(η^6 -C₆Me₆)-2-RuB₉H₁₃]³⁸ (the 2-iridadecaborane species has not yet been synthesized but the shielding effects of third-row transition metals are very similar in metalladecaborane clusters³⁹), and **9a** is given in Figure 3. The apparent close similarity of the shielding characteristics of compound **9a** and decaborane may be due to competing shielding-desielding effects of the metal and sulfur moieties such that they tend to cancel. The relatively low-field resonance due to B(9), however,

(32) (a) Pretzer, W. R.; Rudolph, R. W. *J. Am. Chem. Soc.* **1976**, *98*, 1441. (b) Bown, M.; Fontaine, X. L. R.; Kennedy, J. D. *J. Chem. Soc., Dalton Trans.* **1988**, 1467.

(33) (a) Hilty, T. K.; Thompson, D. A.; Butler, W. M.; Rudolph, R. W. *Inorg. Chem.* **1979**, *18*, 2642. (b) Micciche, R. P.; Briguglio, J. J.; Sneddon, L. G. *Inorg. Chem.* **1984**, *23*, 3992.

(34) Tippe, A.; Hamilton, W. *Inorg. Chem.* **1969**, *8*, 464.

(35) Hilty, T. K.; Rudolph, R. W. *Inorg. Chem.* **1979**, *18*, 1106.

(36) Reference 26, p 268.

(37) Barton, L.; Onak, T. P.; Rimmel, R. J.; Shore, S. G. *Gmelin Handbook of Inorganic Chemistry, Boron Compounds 20*, Springer Verlag: Berlin, 1979 (New Supplement Series Vol. 54), 134 and references therein.

(38) Bown, M.; Fontaine, X. L. R.; Greenwood, N. N.; Kennedy, J. D.; MacKinnon, P. *J. Chem. Soc., Chem. Commun.* **1987**, 817.

(39) Bown, M.; Fontaine, X. L. R.; Greenwood, N. N.; Kennedy, J. D. *J. Organomet. Chem.* **1987**, *325*, 233.

(31) Hawthorne, M. F. *Mol. Struct. Energetics* **1986**, *5*, 225.

Table 7. ^{11}B , ^1H , and ^{31}P ^a NMR Data (in ppm) for *nido*-[(PMe_3)₂H-2,6-IrSB₈H₁₀] (**9a**) in CDCl_3 Solution at 298 K and [(PMe_3)₂Cl-2,6-IrSB₈H₁₀] (**9b**) in $\text{CD}_3\text{C}_6\text{D}_5$ at 373 K with *nido*-SB₉H₁₁ Data for Comparison (CD_2Cl_2)³²

assgnt	compd 9a			compd 9b		SB ₉ H ₁₁	
	$\delta(^{11}\text{B})^b$	$\delta(^1\text{H})^b$	(^{11}B - ^{11}B) COSY correlms (323 K)	$\delta(^{11}\text{B})^b$ (373 K)	$\delta(^1\text{H})^b$ (373 K)	$\delta(^{11}\text{B})$	$\delta(^1\text{H})$
9	+24.1 ^c	+5.49	(4) <i>s</i>	+24.6	+5.55	+17.7	+3.88
1,3	+12.6 (2)	+4.11 (2)	(8, 9, 10) <i>s</i>	+10.0 (2)	+4.06 (2)	+6.6 (2)	+3.55 (2)
5,7	+11.4 (2)	+3.37 (2)	(1, 3) <i>s</i> (8,10) <i>w</i>	+12.0 (2)	4.00 (2)	+25.3 (2)	+5.04 (2)
8,10	-5.5 (2) ^c	+2.88 (2)	(1, 3) <i>s</i>	-7.5 (2)	+3.01 (2)	-9.9 (2)	+2.64(2)
4	-32.7	+0.97	(1, 3, 8, 9, 10) <i>s</i>	-32.3	+1.40	-21.5	+1.76
2	Ir			Ir		-30.7	+0.64
(8,9), (9,10) (CH ₃)		-1.46 (2)			-1.74 (2)		-2.86 (2)
		+1.76 ^d			+1.71 ^d		

^a ^{31}P NMR data in ppm (CDCl_3 , 213 K): -42.7 (*s*) ppm for compound **7a** and -30.0 (*d*), -35.99 (*d*) [$^2J = 11.3$ Hz] ppm for compound **9b** (CDCl_3 , 233 K). ^b Boron and proton resonances related by ^1H - $\{^{11}\text{B}(\text{selective})\}$ spectroscopy. Relative intensities in parentheses. ^c ^1H - $\{^{11}\text{B}(\text{selective})\}$ irradiation of this resonance causes sharpening of bridging protons resonance at $\delta(^1\text{H}) - 1.46$ ppm. ^d Doublet $^2J(^{31}\text{P}-^1\text{H})$ 9.6 Hz (**9a**), 10.3 (**9b**).

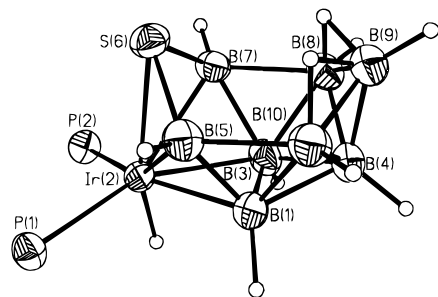


Figure 2. Molecular structure of *nido*-[2,2,2-(PMe_3)₂H-2,6-IrSB₈H₁₀] (compound **9a**) with 50% probability thermal ellipsoids and with methyl groups omitted for clarity. All terminal and bridging boron hydrogen atoms were located and refined satisfactorily. The terminal metal hydride was located from the X-ray data but was refined in a fixed position.

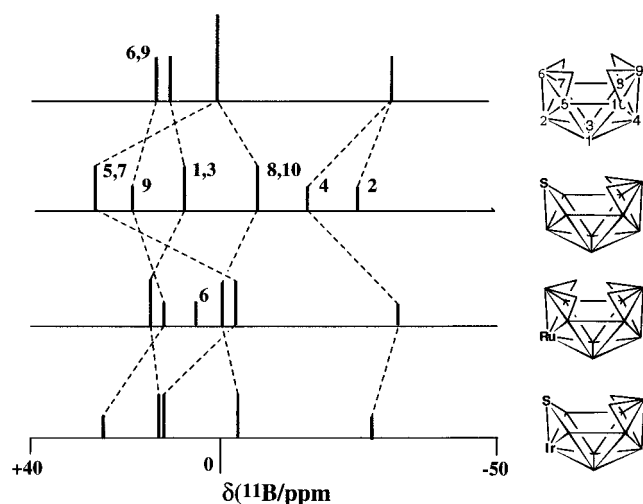


Figure 3. Stick diagram for the ^{11}B NMR positions for *nido*-B₁₀H₁₄,³⁷ *nido*-SB₉H₁₁,³² *nido*-[(η^6 -C₆Me₆)RuB₉H₁₃],³⁸ and *nido*-[2,2,2-(PMe_3)₂H-2,6-IrSB₈H₁₀] (**9a**).

appears result from an additive antipodal deshielding effect of both nuclei.⁴⁰ Antipodal effects are also noted in compounds **10** and **12** described below.

Although compound **9a** and the *arachno*-platinathiaborane compounds are formally isoelectronic species with the metal vertices each contributing two electrons to the cluster bonding, the two metal fragments are not, however, isolobal. The two-orbital, two-electron $\{(\text{PPh}_3)_2\text{-}$

Pt} moiety prefers to take up a 3-connected 6-position compared to the three-orbital, two-electron $\{(\text{PMe}_3)_2\text{-HIr}\}$ moiety which occupies the five-connected 2-position, and the compounds are thus an interesting example of the structural variance which may occur in clusters containing cluster fragments which are formally isoelectronic but not isolobal. The platinathiaborane could be considered to be two electrons short for the required $2n + 6$ skeletal electron count where n is the number of vertices.⁴¹ This phenomenon is now quite common for metallaborane clusters containing the L_2M moiety (where M = Pt or Pd). Examples of "anomalous" electron counts in other platina- and palladaboranes include [5,6-Me₂-7,7-(PEt₃)₂-7,5,6-PtC₂B₄H₄]⁴² and [7,7-(PMe₂Ph)₂-7-PtB₁₀H₁₂],⁴³ [(PPh₃)₂(CO)Os(PhMe₂P)-ClHPtB₅H₇],⁴⁴ and [$\{\text{PhCH}_2\text{NMe}_3\}_2(\text{B}_{10}\text{H}_{12})_2\text{Pd}\cdot\text{MeCN}$]⁴⁵ and related systems, and attempts have been made to account for the discrepancies in the latter systems using molecular orbital calculations.⁴⁶ Again this phenomenon in [7,7-(PMe₂Ph)₂-7-PtB₁₀H₁₂] may be ascribed to be due to the Pt moiety functioning as a two orbital two electron donor and adopting effectively a square-planar configuration although contributions from higher valence Pt(IV) states have been proposed in these systems.^{43,47}

A second compound isolated from the reaction mixture from which **9a** was obtained, *closo*-[2,2,2-(PMe_3)₂H-2,1-IrSB₈H₈] (compound **10**, 7% yield), was also characterized by NMR spectroscopy (Table 9) and by a single-crystal X-ray diffraction study. A projection view of the structure is shown in Figure 4 and selected interatomic dimensions are listed in Table 8. The cluster is seen to be based upon the conventional bicapped Archimedean antiprism in which sulfur occupies an apical position as also observed for the heteroborane analogue *closo*-

(41) (a) Wade, K. *Adv. Inorg. Chem. Radiochem.* **1976**, *18*, 1. (b) Mingos, D. M. P. *Acc. Chem. Res.* **1984**, *17*, 311.

(42) Barker, G. K.; Green, M.; Onak, T. P.; Stone, F. G. A.; Ungermann, C. B.; Welch, A. J. *J. Chem. Soc., Chem. Commun.* **1980**, 1186.

(43) Boocock, S. K.; Greenwood, N. N.; Kennedy, J. D.; McDonald, W. S.; Staves, J. *J. Chem. Soc., Dalton Trans.* **1981**, 2573.

(44) Bould, J.; Crook, J. E.; Greenwood, N. N.; Kennedy, J. D. *J. Chem. Soc., Dalton Trans.* **1991**, 185.

(45) McGregor, S. A.; Scanlan, J. A.; Yellowlees, L. J.; Welch, A. J. *Acta Crystallogr.* **1991**, *C47*, 513.

(46) Macgregor, S. A.; Wynd, A. J.; Moulden, N.; Gould, R. O.; Taylor, P.; Yellowlees, L. J.; Welch, A. J. *J. Chem. Soc., Dalton Trans.* **1991**, 3317.

(47) Boocock, S. K.; Greenwood, N. N.; Hails, M. J.; Kennedy, J. D.; McDonald, W. S. *J. Chem. Soc., Dalton Trans.* **1981**, 1415.

(40) Hermanek, S. *Chem. Rev.* **1992**, *92*, 325 and references therein.

Table 8. Selected Interatomic Distances (Å) and Angles (deg) for **10**

Ir(2)–B(7)	2.255(11)	Ir(2)–B(6)	2.263(12)
Ir(2)–P(1)	2.304(3)	Ir(2)–P(2)	2.304(3)
Ir(2)–B(3)	2.322(11)	Ir(2)–B(5)	2.329(12)
Ir(2)–S(1)	2.365(3)	Ir(2)–H(2)	1.68
S(1)–B(4)	1.91(2)	S(1)–B(5)	1.957(13)
S(1)–B(3)	1.974(12)	B(3)–B(8)	1.80(2)
B(3)–B(7)	1.84(2)	B(3)–B(4)	1.93(2)
B(4)–B(8)	1.76(2)	B(4)–B(9)	1.74(2)
B(5)–B(6)	1.86(2)	B(4)–B(5)	1.91(2)
B(6)–B(10)	1.66(2)	B(5)–B(9)	1.80(2)
B(6)–B(7)	1.90(2)	B(6)–B(9)	1.86(2)
B(7)–B(10)	1.68(2)	B(7)–B(8)	1.87(2)
B(8)–B(9)	1.84(2)	B(8)–B(10)	1.70(2)
B(9)–B(10)	1.71(2)		
B(7)–Ir(2)–B(6)	49.9(4)	B(7)–Ir(2)–P(1)	104.0(3)
B(6)–Ir(2)–P(1)	152.0(3)	B(7)–Ir(2)–P(2)	149.9(3)
B(6)–Ir(2)–P(2)	103.8(3)	P(1)–Ir(2)–P(2)	97.59(10)
B(7)–Ir(2)–B(3)	47.4(5)	B(6)–Ir(2)–B(3)	78.7(4)
P(1)–Ir(2)–B(3)	89.8(3)	P(2)–Ir(2)–B(3)	154.4(3)
B(7)–Ir(2)–B(5)	79.4(4)	B(6)–Ir(2)–B(5)	47.7(4)
P(1)–Ir(2)–B(5)	149.7(3)	P(2)–Ir(2)–B(5)	92.4(3)
B(3)–Ir(2)–B(5)	70.1(4)	B(7)–Ir(2)–S(1)	91.9(3)
B(6)–Ir(2)–S(1)	91.6(3)	P(1)–Ir(2)–S(1)	100.41(11)
P(2)–Ir(2)–S(1)	104.63(11)	B(3)–Ir(2)–S(1)	49.8(3)
P(1)–Ir(2)–H(2)	77.80(8)	B(5)–Ir(2)–S(1)	49.3(3)
B(3)–Ir(2)–H(2)	129.6(3)	P(2)–Ir(2)–H(2)	75.96(9)
B(6)–Ir(2)–H(2)	89.9(3)	B(5)–Ir(2)–H(2)	132.5(3)
S(1)–Ir(2)–H(2)	178.19(7)	B(7)–Ir(2)–H(2)	88.3(3)
B(4)–S(1)–B(5)	59.2(5)	B(4)–S(1)–B(3)	59.3(6)
B(5)–S(1)–B(3)	85.6(5)	B(4)–S(1)–Ir(2)	99.4(4)
B(5)–S(1)–Ir(2)	64.4(4)	B(3)–S(1)–Ir(2)	64.0(3)
B(8)–B(3)–B(4)	61.9(8)	B(8)–B(3)–B(4)	56.4(7)
B(7)–B(3)–B(4)	101.6(8)	B(8)–B(3)–S(1)	113.4(7)
B(7)–B(3)–S(1)	121.0(6)	B(4)–B(3)–S(1)	58.8(6)
B(8)–B(3)–Ir(2)	112.7(7)	B(7)–B(3)–Ir(2)	64.4(5)
B(4)–B(3)–Ir(2)	100.6(6)	S(1)–B(3)–Ir(2)	66.2(3)
B(9)–B(4)–B(8)	63.3(8)	B(9)–B(4)–B(5)	58.6(7)
B(8)–B(4)–B(5)	102.2(9)	B(9)–B(4)–S(1)	118.1(8)
B(8)–B(4)–S(1)	118.2	B(5)–B(4)–S(1)	61.5(6)
B(9)–B(4)–B(3)	101.6(9)	B(8)–B(4)–B(3)	58.2(7)
B(5)–B(4)–B(3)	88.2(7)	S(1)–B(4)–B(3)	61.9(6)
B(9)–B(5)–B(6)	61.2(7)	B(9)–B(5)–B(4)	56.0(7)
B(6)–B(5)–B(4)	100.7(8)	B(9)–B(5)–S(1)	113.4(7)
B(6)–B(5)–S(1)	120.8(8)	B(4)–B(5)–S(1)	59.3(6)
B(9)–B(5)–Ir(2)	112.1(7)	B(6)–B(5)–Ir(2)	64.3(5)
B(4)–B(5)–Ir(2)	100.7(6)	S(1)–B(5)–Ir(2)	66.3(4)
B(10)–B(6)–B(9)	57.7(8)	B(10)–B(6)–B(5)	110.7(9)
B(10)–B(6)–B(7)	55.6(7)	B(5)–B(6)–B(9)	57.8(7)
B(9)–B(6)–B(7)	89.6(7)	B(5)–B(6)–B(7)	102.1(8)
B(5)–B(6)–Ir(2)	68.0(5)	B(10)–B(6)–Ir(2)	118.8(8)
B(7)–B(6)–Ir(2)	64.8(5)	B(9)–B(6)–Ir(2)	112.4(7)
B(10)–B(7)–B(3)	109.9(9)	B(10)–B(7)–B(8)	56.7(8)
B(3)–B(7)–B(8)	58.0(7)	B(10)–B(7)–B(6)	54.9(6)
B(3)–B(7)–B(6)	101.8(7)	B(8)–B(7)–B(6)	88.5(7)
B(10)–B(7)–Ir(2)	118.6(7)	B(3)–B(7)–Ir(2)	68.2(5)
B(8)–B(7)–Ir(2)	112.7(7)	B(6)–B(7)–Ir(2)	65.3(5)
B(10)–B(8)–B(3)	111.0(8)	B(10)–B(8)–B(4)	111.8(10)
B(10)–B(8)–B(9)	57.7(8)	B(4)–B(8)–B(3)	65.4(7)
B(3)–B(8)–B(9)	102.9(8)	B(4)–B(8)–B(9)	57.8(8)
B(4)–B(8)–B(7)	106.7(8)	B(10)–B(8)–B(7)	55.8(7)
B(9)–B(8)–B(7)	91.1(8)	B(3)–B(8)–B(7)	60.1(6)
B(10)–B(9)–B(4)	112.0(10)	B(10)–B(9)–B(5)	111.6(9)
B(4)–B(9)–B(5)	65.4(8)	B(10)–B(9)–B(8)	56.9(8)
B(4)–B(9)–B(8)	58.9(7)	B(5)–B(9)–B(8)	103.9(8)
B(10)–B(9)–B(6)	55.4(7)	B(4)–B(9)–B(6)	107.4(8)
B(5)–B(9)–B(6)	61.1(7)	B(8)–B(9)–B(6)	90.8(8)
B(6)–B(10)–B(8)	103.3(9)	B(6)–B(10)–B(7)	69.5(7)
B(6)–B(10)–B(9)	66.9(8)	B(7)–B(10)–B(8)	67.5(8)
B(8)–B(10)–B(9)	65.4(9)	B(7)–B(10)–B(9)	103.0(9)

[SB₉H₉]⁴⁸ with the iridium in an adjacent equatorial position. The compound is, as far as we are aware, the first *closo*-metallathiadecaborane cluster to be synthe-

Table 9. ¹¹B, ¹H, and ³¹P^a NMR Data (in ppm) for *closo*-[2,2,2-(PMe₃)₂H-2,1-IrSB₈H₈] (**10**)

assgnt ^c	δ(¹¹ B) ^b (373 K)	J(B–H)/ Hz	δ(¹ H) ^b (297 K)	(¹¹ B– ¹¹ B) COSY correlns (323 K)
10	+68.8	150	+9.0	(b, d) <i>s</i>
3,5 (a)	–0.86(2)	150	+2.72 (2)	(10, b, c) <i>s</i>
4 (a)	–0.86	150	+3.27	
(6,7) or (8,9) (b)	–9.0(2)	160	+0.80 (2)	(a) <i>s</i> , (c) <i>m</i>
(8,9) or (6,7) (c)	–30.2(2)	160	–1.28 (2)	(10, a) <i>s</i> , (b) <i>m</i>
H(2)			–9.51 ^d	
(CH ₃)			+1.70 ^e	

^a ³¹P NMR data in ppm (CDCl₃, 213 K): –31.6 (*s*) ppm. ^b Boron and proton resonances related by ¹H–{¹¹B(selective)} spectroscopy. Relative intensities greater than unity in parentheses. ^c Letters identify resonances for (¹¹B–¹¹B) COSY purposes. See last column in this table. ^d Triplet, ²J(³¹P–¹H) *cis* 24.9 Hz. ^e Doublet, ²J(³¹P–¹H) 10.2 Hz.

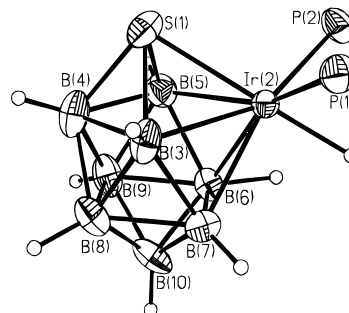


Figure 4. Molecular structure of *closo*-[2,2,2-(PMe₃)₂H-2,1-IrSB₈H₈] (compound **10**) with 50% probability thermal ellipsoids and with methyl groups omitted for clarity. All terminal boron hydrogen atoms were located and refined satisfactorily. The terminal metal hydride was located from the X-ray data and refined in a fixed position.

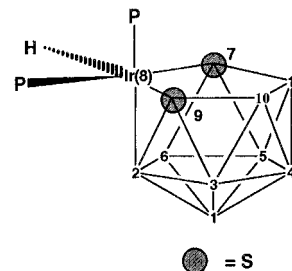


Figure 5. Proposed structure of *nido*-[8,8,8-(PMe₃)₂H-8,7,9-IrS₂B₈H₈] (**11a**).

sized, but it is of interest to note that an isostructural iridacarbododecaborane cluster⁵ with a similar apical (C)–equatorial (Ir) arrangement has been isolated in low yield where the carbon vertex was introduced via cluster incorporation of the methanol reaction solvent. We were unable to assign the NMR spectra completely although the boron resonance due to the apical B(10) vertex appears at very low field (+68.8 ppm) and is comparable to that found in *closo*-[SB₉H₉] (+74.5 ppm) which results from the antipodal deshielding effect of the sulfur.⁴⁸

The third and major component of the reaction, isolated in 20% yield, was tentatively identified as the 11-vertex cluster *nido*-[7,7,7-(PMe₃)₂H-8,7,9-IrS₂B₈H₈] (**11a**, Figure 5) by a comparison of its multinuclear magnetic resonance data (Table 10) with those of the structurally characterized rhodadithiaundecaborane *nido*-[7,7,7-(PPh₃)₂H-8,7,9-RhS₂B₈H₈].³⁰ Assignment of the resonances is, again, uncertain as very little coupling information was available from [¹¹B–¹¹B] COSY experiments, but a comparison of the ¹¹B and ¹H NMR

(48) Pretzer, W. R.; Rudolph, R. W. *J. Am. Chem. Soc.* **1973**, *95*, 931.

Table 10. ^{11}B , ^1H , and $^{31}\text{P}^a$ NMR Data (in ppm) for *nido*-[(PMe_3) $_2\text{HirS}_2\text{B}_8\text{H}_8$] (**11a**) and *nido*-[(PMe_3) $_2\text{ClIrS}_2\text{B}_8\text{H}_8$] (**11b**) in CDCl_3 Solution at 298 K with Comparison Data for *nido*-[(PPh_3) $_2\text{HRhS}_2\text{B}_8\text{H}_8$] 30

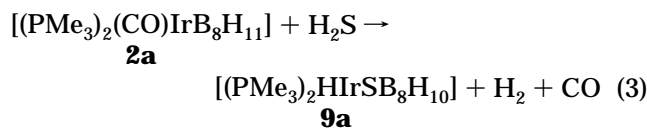
assgnt ^f	compd 11a				compd 11b		[(PPh_3) $_2\text{HRhS}_2\text{B}_8\text{H}_8$]	
	$\delta(^{11}\text{B})^b$	$J(\text{B}-\text{H})/\text{Hz}$	$\delta(^1\text{H})^b$	($^{11}\text{B}-^{11}\text{B}$) COSY correlns (323 K)	$\delta(^{11}\text{B})^b$	$\delta(^1\text{H})^b$	$\delta(^{11}\text{B})^b$	$\delta(^1\text{H})^b$
a	+12.9	141	+6.09	(e, f) s, (g) m	+13.1	+5.92	+12.0	+4.07
2 or 6	+3.2	151	+3.12 ^e	(c) s, (g) s	+5.4	+3.93 ^k	+3.4 (2)	+3.53, +3.35
6 or 2	-0.7	169	+3.51	(b) s, (g) s	+6.6	+3.75		
d	-5.7(2)	<i>i</i>	+2.97, +2.85		-5.1 (2)	+2.63, +3.14	-4.1 (2)	+2.46, +2.05
e	-13.8	169	+2.53	(g) s	-15.6	+2.88	-13.7	+2.00
f	-16.9	160	+2.55	(g) s	-16.2	+2.23	-16.8	+2.03
l	-32.9	141	+1.68	(a) m (b, c, d, e, f) s	-32.5	+1.65	-28.1	+1.72
H(2) (CH_3)	-32.9		-14.26 ^d +1.85, ^g +1.75 ^h			+1.83, +1.74 ^l		-11.98

^a ^{31}P NMR data in ppm (CDCl_3 , 213 K): -28.0 (*d*), -37.9 (*d*) [$^2J = 10.8$ Hz] ppm for compound **11a** and -31.6 (*s*) ppm for compound **11b**. ^b Boron and proton resonances related by $^1\text{H}-\{^{11}\text{B}(\text{selective})\}$ spectroscopy. Relative intensities in parentheses. ^d Doublet of doublets $^2J(^{31}\text{P}-^1\text{H})$ *cis* 18.7, 23.7 Hz. ^e Doublet, $J = 15.6$ Hz. ^f Triplet, $^2J(^{31}\text{P}-^1\text{H})$ *cis* 24.9 Hz. ^g Doublet, $^2J(^{31}\text{P}-^1\text{H})$ 10.2 Hz. ^h Doublet, $^2J(^{31}\text{P}-^1\text{H})$ 10.8 Hz. ⁱ Boron resonance too broad to exhibit coupling to terminal proton. ^j Letters identify resonances for ($^{11}\text{B}-^{11}\text{B}$) COSY purposes. ^k Doublet, $^2J(^{31}\text{P}-^1\text{H})$ 13 Hz. ^l Both doublets, $^2J(^{31}\text{P}-^1\text{H})$ 10 Hz.

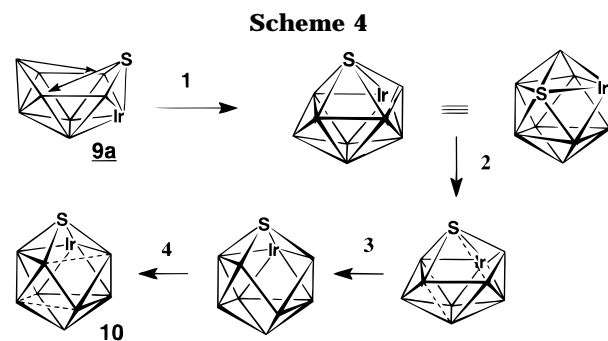
chemical shift data with those of the rhodadithiaundecaborane species shows a striking similarity giving us a high degree of confidence in the proposed structure. Attempts to confirm the proposed structure with an X-ray diffraction study were unsuccessful as crystals showed an unresolvable positional disorder.

Finally, it may be noted that compounds **9a**, **10**, and **11a** were found to react slowly and cleanly at room temperature with the CDCl_3 NMR solvent, and more rapidly at elevated temperatures, effecting a replacement of the terminal iridium hydride with Cl. A solution of **9a** in CDCl_3 at 50 °C for 4 days showed 60% conversion (by integrated ^{11}B NMR spectroscopy) to *nido*-[2,2,2-(PMe_3) $_2\text{Cl}-2,6\text{-IrSB}_8\text{H}_{10}$] (compound **9b**). Correspondingly, compound **11a** gave *nido*-[7,7,7-(PMe_3) $_2\text{Cl}-8,7,9\text{-IrS}_2\text{B}_8\text{H}_8$] (compound **11b**). NMR data are listed in Tables 7 and 10, respectively. **10** was also noted to react similarly, but the chloro species was not isolated.

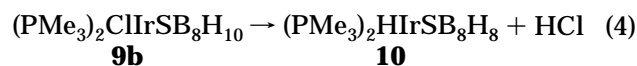
Compound **9a** clearly results, after initial dihydrogen loss in the *arachno*-**1a** \rightarrow *nido*-**2a** step, from addition of H_2S to the *nido*-iridanonaborane according to eq 3.



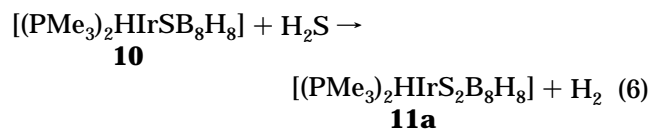
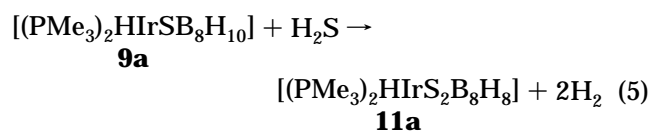
Unlike the case of alkyne addition it is not possible to postulate a straight-forward addition of sulfur to the cluster which would give the observed positions of S and Ir in the product and a cluster rearrangement seems likely. Further dihydrogen elimination from **9a** would then, in principle, yield the *closo*-metallathiaaborane species **10**. Interestingly, pyrolysis of *nido*-[6- SB_9H_{11}] at 450 °C leads to *closo*-[1- SB_9H_9].⁴⁸ As pointed out by Pretzer and Rudolph,⁴⁸ a simple closure step of the *nido* cluster would not result in an apical position for the S atom in the *closo* species or, in the case of **9a**, in the observed 2,3 position for the sulfur and iridium vertices in **10** (Step 1, Scheme 4).^{32a} However, in the manner proposed by Pretzer and Rudolph to account for the apical heteroatom disposition in the *closo*-thiadecaborane, a diamond-square-diamond rearrangement on two faces would also result in the observed S(1) and Ir(2) dispositions in compound **10** (steps 2 to 4, Scheme 4). We have not observed any tendency for H_2 loss directly



in **9a** at the temperatures reached during NMR spectroscopic investigation of the species (up to *ca.* 90 °C) although it may be noted that high-resolution mass spectroscopic measurements on the chloro-substituted compound **9b** showed two ion envelopes of relative intensities 40:100 with the former being due to the parent ion with loss of H [m/q 508.1422 (obsd), 508.1410 (calcd)] and the latter, more intense envelope corresponding to the parent ion mass with loss of HCl [m/q 472.1724 (obsd), 472.1736 (calcd)]. This corresponds to the calculated mass for compound **10** suggesting that the *closo* species could be formed in the mass spectrometer as shown in eq 4. Further reaction with H_2S must



take place with either **9a** or **10** to afford the metalladithiaaborane species **11a** again with H_2 -elimination (eqs 5 and 6). This two-stage heteroatom cluster assembly



process contrasts with that of the one-boron atom degradation process from an unisolated metalla- S_2B_9 intermediate which gives the rhodium analogue.³⁰

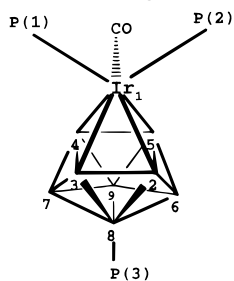
Reaction in the iridanonaborane system appears to proceed in alternate directions depending on the nature of the substituent in the iridanonaborane [(CO)(PMe₃)₂-IrB₈H₁₀X] (compound **2**). When X = H (**2a**) the cluster, on thermolysis, undergoes condensation to afford the species [(PMe₃)₂(CO)Ir]₂B₁₆H₁₄ (**4**)⁹ with retention of CO or it degrades completely. If X = Cl (**2b**), it goes on to form *isocloso*-(PMe₃)₂HB₈H₇Cl (**3**).^{8a} It appears that, after CO loss, unless there is a suitable reactant present with which to form a more thermally stable species, the system with X = H falls apart. Thus, with H₂S or with alkynes reaction takes place to afford a series of products which are the result of heteroatom incorporation. Interestingly, reaction of **2a** with excess B₁₀H₁₄ in refluxing xylene affords the unsubstituted *isocloso*-(PMe₃)₂HirB₈H₈ in up to 16% yield⁴⁹ and therefore the unisolated 50% of starting metallaborane may also play a role in some of these reactions whereas reaction with C₂H₄ affords a low yield of a product which NMR and IR spectra suggest is *isonido/closo*-(PMe₃)₂(CO)IrB₈H₇(PMe₃).⁵⁰ Clearly the system is complex and the potential role of the unisolated 50% of starting metallaborane cannot be discounted.

The proximity of the heteroatoms and the metal centers in the metallacarborane and metallathiorborane products implies that the metal is intimately involved in the process although similar reactions of non-metal-containing borane clusters allow other possibilities. Examples include the classical reaction of C₂H₂ with L₂B₁₀H₁₂ to form C₂B₁₀H₁₂,⁵¹ the addition of nitriles to SB₉H₁₁ to afford monocation heteroborane species,⁵² and the synthesis of cobaltthiaboranes from H₂S in a metal atom vapor reactor.²

Metallaazaborane. Reaction of **1** with a 10-fold molar excess of anhydrous hydrazine in refluxing xylene, followed by chromatographic separation of the products, gave a *ca.* 10% yield of the iridaazaborane cluster *nido*-[2,2,2-(PMe₃)₃-2,9-IrNB₇H₉] (compound **12**) identified by NMR spectrometry (Table 12), high-resolution mass spectroscopy, and a single-crystal X-ray diffraction study. Figure 6 shows a projection of the

(49) Bould, J.; Barton, L. Unpublished results.

(50) The data for the compound *isonido/closo*-(PMe₃)₂(CO)IrB₈H₇(PMe₃) are as follows. NMR shifts in ppm (CDCl₃ at 300 K) are given in the order assignment, δ(¹H) [(δ¹H) of directly attached hydrogen atom in square brackets] and are as follows: B(4,5) +24.1 [+5.52], B(2,3) -1.2 [+3.35, doublet of doublets ⁿJ = *ca.* 6.5 Hz], B(8) -18.2 [doublet, ²J(B-P) 184 Hz], B(6,7) -21.9 [+1.00], B(9) -30.3 [-0.85]; PMe₃ on iridium +1.64 [²J(P-H) = 16.0 Hz], on B(8), +1.72 [²J(P-H) = 19.5 Hz]; δ(³¹P) (CDCl₃ at 223 K) P(1,2) -49.8 sharp, P(3) -7.9 vbr. IR (3M Teflon IR card)/cm⁻¹: ν(CO) 1964 s, ν(BH) 2462 s. The data are consistent with the following structure:



(51) Heying, T. L.; Ager, J. W., Jr.; Clark, S. L.; Mangold, D. J.; Goldstein, H. L.; Hillman, M.; Polak, R. J.; Szymanski, J. W. *Inorg. Chem.* **1963**, *2*, 1089.

(52) Kang, S. O.; Furst, G. T.; Sneddon, L. G. *Inorg. Chem.* **1989**, *28*, 2339.

(53) (a) Schneider, L.; Englert, U.; Paetzold, P. Z. *Anorg. Allg. Chem.* **1994**, *620*, 1191. (b) Arafat, A.; Baer, J.; Huffman, J. C.; Todd, L. J. *Inorg. Chem.* **1986**, *25*, 3757.

Table 11. Selected Interatomic Distances (Å) and Angles (deg) for **12**

Ir(2)-B(1)	2.06(5)	B(3)-B(7)	1.84(9)
Ir(2)-B(6)	2.13(5)	B(3)-B(4)	1.83(8)
Ir(2)-B(3)	2.19(6)	B(4)-B(7)	1.75(8)
Ir(2)-P(1)	2.232(14)	B(4)-B(8)	1.81(7)
Ir(2)-P(2)	2.307(13)	B(4)-B(5)	1.85(7)
Ir(2)-P(3)	2.309(11)	B(5)-B(8)	1.75(9)
Ir(2)-B(5)	2.51(6)	B(6)-N(9)	1.47(7)
B(1)-B(3)	1.63(7)	B(6)-B(7)	1.81(9)
B(1)-B(4)	1.74(7)	B(7)-N(9)	1.48(8)
B(1)-B(5)	1.93(7)	B(7)-B(8)	1.77(10)
B(3)-B(6)	1.84(6)	B(8)-N(9)	1.44(8)
B(1)-Ir(2)-B(6)	88(2)	B(1)-B(3)-Ir(2)	63(3)
B(1)-Ir(2)-B(3)	45(2)	B(6)-B(3)-Ir(2)	63(2)
B(6)-Ir(2)-B(3)	50(2)	B(7)-B(3)-Ir(2)	111(3)
B(1)-Ir(2)-P(1)	102.4(13)	B(4)-B(3)-Ir(2)	102(3)
B(6)-Ir(2)-P(1)	99.5(14)	B(8)-B(5)-Ir(2)	101(3)
B(3)-Ir(2)-P(1)	85(2)	B(4)-B(5)-Ir(2)	91(3)
B(1)-Ir(2)-P(2)	88.7(14)	B(1)-B(5)-Ir(2)	53(2)
B(6)-Ir(2)-P(2)	165.1(14)	N(9)-B(6)-B(7)	52(3)
B(3)-Ir(2)-P(2)	131.9(14)	N(9)-B(6)-B(3)	107(4)
P(1)-Ir(2)-P(2)	95.4(5)	N(9)-B(6)-Ir(2)	119(4)
B(1)-Ir(2)-P(3)	159.1(13)	B(7)-B(6)-Ir(2)	116(3)
B(6)-Ir(2)-P(3)	81.3(14)	B(3)-B(6)-Ir(2)	67(2)
B(3)-Ir(2)-P(3)	131.0(14)	N(9)-B(7)-B(4)	107(5)
P(1)-Ir(2)-P(3)	97.2(5)	N(9)-B(7)-B(8)	52(3)
P(2)-Ir(2)-P(3)	96.7(4)	B(4)-B(7)-B(8)	62(3)
B(1)-Ir(2)-B(5)	49(2)	N(9)-B(7)-B(6)	52(4)
B(6)-Ir(2)-B(5)	79(2)	N(9)-B(7)-B(3)	106(5)
B(3)-Ir(2)-B(5)	71(2)	N(9)-B(8)-B(7)	54(4)
P(1)-Ir(2)-B(5)	150.9(12)	N(9)-B(8)-B(5)	117(6)
P(2)-Ir(2)-B(5)	88.4(14)	N(9)-B(8)-B(4)	106(5)
P(3)-Ir(2)-B(5)	111.1(11)	B(8)-N(9)-B(7)	75(5)
B(3)-B(1)-Ir(2)	72(3)	B(8)-N(9)-B(6)	116(5)
B(4)-B(1)-Ir(2)	111(3)	B(7)-N(9)-B(6)	76(4)
B(5)-B(1)-Ir(2)	78(2)		

molecule. Selected interatomic distances and angles are listed in Table 11. The quality of the X-ray data were low due to decomposition of the crystal in the X-ray beam such that only heavy atoms were located and with high estimated standard deviations. However, together with the other data, the cluster is unambiguously seen to be a *nido*-nine vertex cluster based on the bicapped Archimedean antiprism of *closo*-[NB₉H₁₀]⁵³ with an equatorial boron vertex missing and is thus isostructural with the probable precursor *nido*-[(PMe₃)₂(CO)-IrB₈H₁₁]^{8b} (**2a**; see Scheme 1 and Figure 8) and with *nido*-[B₉H₁₂]⁻.⁵⁴ There are similar azaboranes in the literature which do not contain metals. For example, concurrent with this work, substituted derivatives of the azaborane analogue *nido*-NB₈H₁₁, RNB₈H₉ (R = *p*-ClC₆H₄, *p*-MeC₆H₄, PhCH₂) were reported⁵⁵ and an *arachno*-azanaborane, NB₈H₁₃, was synthesized and structurally characterized some time ago.⁵⁶ The position of the heteroatom N(9) in the *pseudo*-apical position is clear from the significantly shorter interatomic distances of 1.44(8)–1.47(7) Å to that vertex compared to the boron–boron distances [1.63(7)–1.93(7) Å] and is in the position that might be expected for an NH moiety which is subrogating a HB(H_{bridging})₂ unit in the iridanonaborane congener. The distances, allowing for the large estimated standard deviations, are in line with those in other azaboranes.^{53a,56,57} The dimensions associated with the iridium environment are quite similar

(54) Jacobsen G. B.; Meina, D. G.; Morris, J. H.; Thomson, C.; Andrews, S. J.; Reed, D.; Welch, A. J.; Gaines, D. F. *J. Chem. Soc., Dalton Trans.* **1985** 1645.

(55) Roth, M.; Paetzold, P. *Chem. Ber.* **1995**, *128*, 1221.

(56) Base, K.; Plessek, J.; Hermanek, S.; Huffman, J.; Ragatz, P.; Schaeffer, R. *J. Chem. Soc., Chem. Commun.* **1975**, 934.

Table 12. ^{11}B , ^1H , and ^{31}P ^a NMR Data for *nido*-[(PMe₃)₃IrNB₇H₉] (**11**) in CDCl₃ (298 K) Solution and Comparison Data for *nido*-[(PMe₃)₂(CO)IrB₈H₁₁] (**2**) (CDCl₃ Solution, 298 K)^{b,28}

[(PMe ₃) ₃ IrNB ₇ H ₉] (11)				[(PMe ₃) ₂ (CO)IrB ₈ H ₁₁] (2a)		
assgnt	$\delta(^{11}\text{B})$	$\delta(^1\text{H})^b$	$J(\text{B}-\text{H})$	assgnt	$\delta(^{11}\text{B})$	$\delta(^1\text{H})^b$
1	+41.2	+6.44	156	1	+23.1	+5.04
6	+4.2	+3.70	136	4	+8.8	+4.90
4 ^c	-1.3	+4.14	152	6	-5.3	+2.94
8	-2.8	+1.96	147	8	-13.6	+1.02
9 ^d				9	-14.5	+2.99
3	-23.6	+0.49 ^e	130	3	-15.3	+0.83
7	-43.6	-0.55	151	5	-39.9	-0.51
5	-54.6	-2.30	<i>f</i>	7	-52.5	-1.48
H(2,5)		-13.23 ^g		H(2,5)		-14.50 ^h
				H(6,9), (8,9)		-2.10, -2.96
N(H)		+5.12				
P(CH ₃)		+1.68 (9), +1.60 (9), +1.56 (9) ⁱ		P(CH ₃)		+1.76 (9), +1.73 (9) ^j

^a $\delta(^{31}\text{P})$ NMR data in ppm (CDCl₃, 233 K (**12**) and 223 K for [(PMe₃)₂(CO)IrB₈H₁₁]): -40.9 [(*q*), $^2J(^{31}\text{P}-^{31}\text{P})$ 20 Hz or *d,d*, $J = 20$, 40 Hz], -51.9 (*br*), -53.7 (*br*) for compound **12** and -39.5 (*d*), -50.5 (*d*) ($^2J = 19$ Hz) for [(PMe₃)₂(CO)IrB₈H₁₁]. ^b Relative intensities greater than unity in parentheses. ^c Relative assignments are uncertain although the most probable positions are as shown. B(4) is assigned on the basis of the generally sharper linewidths for nonfacial boron atoms *versus* those in the open face of boron clusters (see Figure 7). ^d Site of heteroatom N(9). See Figure 6. ^e Doublet probably due to coupling to phosphorus $^3J(^{31}\text{P}-^1\text{H}) = 22$ Hz. ^f Too broad to measure. ^g $^2J(^{31}\text{P}-^1\text{H})_{\text{trans}} = 57$ Hz. The resonance is also selectively sharpened on irradiation of the boron resonance at $\delta(^{11}\text{B}) = -54.6$ ppm. ^h $^2J(^{31}\text{P}-^1\text{H})_{\text{trans}} = 62$ Hz. ⁱ Doublets, $^2J(^{31}\text{P}-^1\text{H}) = 8, 9$, and 11 Hz, respectively. ^j Doublets, $^2J(^{31}\text{P}-^1\text{H}) = 9.5$ and 10.5 Hz, respectively.

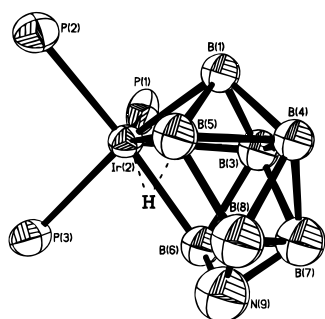


Figure 6. Molecular structure of *nido*-[2,2,2-(PMe₃)₃-2,9-IrNB₇H₉] (compound **12**) with 30% probability thermal ellipsoids and with methyl groups omitted for clarity. All heavy atoms were located. NMR spectroscopy shows terminal hydrogen atoms on all the boron atoms and nitrogen atom N(9) and an additional hydrogen atom bridging Ir(2)–B(5) which is indicated by dashed lines.

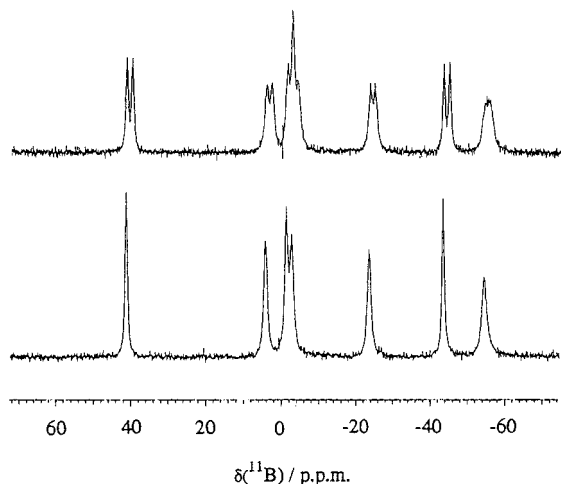


Figure 7. 96 MHz ^{11}B (upper trace) and $^{11}\text{B}\{^1\text{H}\}$ (lower trace) spectra for *nido*-[2,2,2-(PMe₃)₃-2,9-IrNB₇H₉] (compound **12**).

to those in *nido*-[(PMe₃)₂(CO)IrB₈H₁₁]; in particular the Ir(2)–B(5) separation of 2.51(6) Å compares well to that in the iridanonaborane of 2.500(6) Å^{8c} and an analogous rhenanonaborane [(PMe₂Ph)₃H₂ReB₈H₁₁] [2.527(13) Å].²⁸ In each compound the M(2)–B(5) vector is the site of a hydrogen atom bridging the metal and the boron ap-

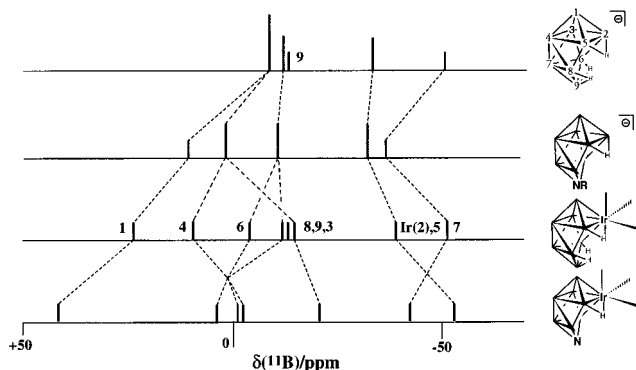


Figure 8. Stick diagram for the ^{11}B NMR positions for the isostructural and effectively isoelectronic series [B₉H₁₂]⁻,⁵⁴ [B₈H₉NR]⁻,⁵⁵ [(PMe₃)₂(CO)IrB₈H₁₁] (**2a**), and *nido*-[2,2,2-(PMe₃)₃-2,9-IrNB₇H₉] (**12**).

proximately *trans* to phosphorus atom P(1). The presence of the bridging hydrogen atom in **12** is apparent from the ^1H NMR spectrum where it appears at quite high field for a bridging H-atom in almost the same position as that in the iridanonaborane again demonstrating the essential similarity of the two species [$\delta(^1\text{H}) = -13.23$ ppm, $^2J(^{31}\text{P}-^1\text{H})_{\text{trans}} = 57$ Hz in compound **12** versus -14.50 ppm, $J = 62$ Hz in **2a**]. Insufficient sample prevented the attainment of useful information from (^{11}B – ^{11}B) COSY experiments, but we are quite confident of our assignments. The atoms B(5) and B(7) are distinguishable on the basis of their relative peak widths and B(3) on the basis of coupling of its exo-terminal proton to ^{31}P . The ^{11}B NMR spectrum of **12** is given in Figure 7 and a ^{11}B chemical shift correlation diagram for **12** and the isostructural and effectively isoelectronic species [B₉H₁₂]⁻,⁵⁴ [B₈H₉NR]⁻,⁵⁵ and [(PMe₃)₂(CO)IrB₈H₁₁] (**2a**) is given in Figure 8. The correlation between the chemical shifts of the metalaborane **2a** and the parent binary borane [B₉H₁₂]⁻ has been described previously.²⁸ The azaboranes fit into the picture quite well. As with the *nido*-iridathiadecaborane, **9a**, the shielding effects of the heteroatom and iridium tend to cancel although in the case of the apical B(10) vertex they appear to be precisely additive such that the chemical shift of that vertex in compound **12** is the resultant of the two shielding effects and the

extent of spreading out of the chemical shifts in **12** is an indication of the opposing effects on the electronic distribution in the molecule of the metal center and the nitrogen heteroatom.⁴⁰

Other species were present in the product mixture although we have been unable to characterize them fully. Clearly the reaction is not clean and involves replacement of the metal carbonyl by phosphine arising from other species in solution (as does compound **6**). However, the overall stoichiometry (equation 7) can be



rationalized by loss of the elements of BH_3 and NH_3 suggesting a simple deboronation of the cluster by base and incorporation of $\{\text{NH}\}$ with no direct role for the metal atom.

Conclusion

Our initial hypothesis that the redox-flexible iridanonorane system would be a suitable substrate for heteroatom incorporations has been shown to be viable. It is clear that with alkynes the reaction occurs directly with the *nido*- rather than the *arachno*-iridanonorane and before carbonyl elimination although whether dihydrogen is lost before or after coordination of the alkyne cannot be determined at this stage. It is tempting to hypothesize that the elimination step provides the coordination vacancy for the ethyne moiety. It is interesting that in all four processes **2** \rightarrow **5**, **2** \rightarrow **9**, **2** \rightarrow **10**, and **2** \rightarrow **11** one, one, two, or three molecules of dihydrogen are eliminated giving an effective incorporation of C_2 , S , S , and S_2 , respectively. In the case of the incorporation of nitrogen the reaction appears to proceed differently. As in the case of the deboronation reactions by amines, reported by Paetzold,⁵⁵ coordination of the N_2H_4 moiety and deboronation by loss of the elements of ammine-borane is followed by incorporation of the remaining N atom. In this case it appears that the presence of the metal is not required and thus the redox flexibility of the starting iridaborane is not important.

The results reported here suggest that further heteroatom incorporation reactions are likely to succeed in this system. Thus reaction with H_2Se , H_2Te , and HCN among other heteroatom reagents may lead to new metallaheteroboranes. Further, it is possible that related metallaborane clusters such as *nido*- $[(\text{PMe}_3)\text{-H}(\text{IrB}_9\text{H}_{13})]^{58}$ may undergo similar reactions. Finally there is the potential to construct novel catalytic systems in this area. The iridaborane system tends to behave differently depending on the identity of cluster substituents and appropriate choice and site of substituent may allow modification of reactions taking place through the metal center, a feature we hope to investigate in the future.

Acknowledgment. We acknowledge the generous support of this work by the National Science Foundation (Grant No. CHE-9311557), the Missouri Research Board and UM—St. Louis for a Research Incentive Award. We also acknowledge the NSF (Grant No. CHE-9318696), the DOE (Grant No. DE-FG02-92CH10499), and the UM—St. Louis Center for Molecular Electronics for grants which allowed purchase of the Varian Unity Plus NMR spectrometer and the latter two along with the NSF (Grant No. CHE-9309690) for funds to purchase the X-ray diffractometer. We also thank Mr. Charles Gloeckner and Dr. Fred Hileman of Monsanto Co. for mass spectra and the Johnson-Matthey Co. for a loan of $\text{IrCl}_3 \cdot 3\text{H}_2\text{O}$.

Supporting Information Available: Listings of atomic coordinates, bond distances and angles, anisotropic displacement parameters, hydrogen coordinates and isotropic displacement parameters, and experimental details for compounds **5a**, **9a**, **10**, and **12** (23 pages). Ordering information is given on any current masthead page. Structure factor tables are available from the authors.

OM960313W

(57) Lomme, P.; Meyer, F.; Englert, U.; Paetzold, P. *Chem. Ber.* **1995**, *128*, 1225.

(58) Bould, J.; Kennedy, J. D.; Greenwood, N. N. *J. Chem. Soc., Dalton Trans.* **1990**, 1451.